Atmospheric Environment 365 (2026) 121668

Contents lists available at ScienceDirect

Atmospheric Environment

journal homepage: www.elsevier.com/locate/atmosenv

The impacts of the Ultra Low Emission Zone (ULEZ) and COVID-19 restrictions on air quality in central London – evidence for an increase in small particles

Douglas J. Gregg [a], Jordan Tompkins [b], Rebecca L. Cordell [a], Andrew S. Brown [b], Kirsty L. Smallbone [c], Joshua D. Vande Hey [d,e], Kevin P. Wyche [c], Paul S. Monks [a,*]

[a] School of Chemistry, University of Leicester, Leicester, LE1 7RH, UK
[b] Air Quality & Aerosol Metrology Group, National Physical Laboratory, Teddington, Middlesex, TW11 0LW, UK
[c] School of Science & Technology, Nottingham Trent University, Nottingham, NG11 8NS, UK
[d] Department of Physics & Astronomy, University of Leicester, Leicester, LE1 7RH, UK
[e] Centre for Environmental Health & Sustainability, University of Leicester, Leicester, LE1 7RH, UK

HIGHLIGHTS

- ULEZ and COVID-19 decreased larger particles and increased nucleation mode particles.
- ULEZ accelerated declines in NO_2, PM_{10}, $PM_{2.5}$ and non-nucleation-mode particles.
- Lockdowns increased O_3 and increased NO_2 via classical O_x couple chemistry.
- Adjusting for weather & traffic confirms policies—not seasonality—drive shifts.
- Policy implications as traffic emission reductions can elevate O_3 and UFP abundance.

ARTICLE INFO

Keywords:
Air pollution interventions
ULEZ
Ultrafine particles
Particle size distribution
Secondary atmospheric pollution

ABSTRACT

Introduced in April 2019, the London Ultra Low Emission Zone (ULEZ) targets reductions in NO_x and PM emissions to improve ambient air quality, with COVID-19 related restrictions superimposed throughout much of 2020 and 2021. However, little existing research assesses the impact of these interventions on O_3 and UFP (Ultrafine particles) concentrations, or accounts for variations in meteorological or anthropogenic influences. To assess these effects, NO_2, O_3, PM_{10}, $PM_{2.5}$ and 51 size-channel UFP data collected between January 2015 and December 2022 were normalised using Boosted Regression Tree (BRT) models comprised of twelve predictor variables, including overall trend, time of day/year, wind speed/direction, temperature and traffic volume. The introduction of the ULEZ expedited reductions in NO_2, PM_{10} and $PM_{2.5}$ abundance, aligning with existing research, alongside reductions in nucleation mode UFP abundance and concomitant increases in O_3, Aitken and accumulation mode UFP abundance. The implementation of COVID-19 restrictions expedited an increase/decrease in O_3/NO_2 respectively through the typical O_X couple chemistry. The use of BRT models accounts for changes in the predictor variables, thereby showing that changes in atmospheric composition are not wholly a reflection of seasonality, meteorology or anthropogenic activity. The findings indicate the introduction of both ULEZ and COVID-19 restrictions precipitated a reduction in ambient concentrations of larger particulate matter (i.e. PM_{10}, and $PM_{2.5}$) and larger modes of UFPs (i.e Accumulation and Aitken), alongside increasing concentrations of nucleation mode particles. The findings reinforce the necessity of examining the impact of interventions on atmospheric composition, including changes in the abundance of secondary pollutants.

* Corresponding author.
E-mail address: paul.monks@leicester.ac.uk (P.S. Monks).

https://doi.org/10.1016/j.atmosenv.2025.121668
Received 18 July 2025; Received in revised form 17 October 2025; Accepted 9 November 2025
Available online 15 November 2025

1. Introduction

In London, UK, reductions in the emissions of certain air pollutants that resulted from the COVID-19 lockdown were superimposed on top of on-going emissions reductions as a result of the implementation of a new Ultra-Low Emissions Zone (ULEZ) to the city, a scheme that was launched in April 2019 and later expanded in October 2021 (London Borough of Hounslow, 2022) and August 2023 (Transport for London, 2022a). Alongside the pre-existing low emission zone (LEZ) designed to reduce diesel emissions from heavy vehicles over 3.5 tonnes in weight (5 tonnes for buses and coaches) (Transport for London, 2025), the ULEZ is designed to reduce emissions from cars, vans and motorcycles, with vehicles that do not meet a specified Euro standard required to pay a fee to drive within the zone (Transport for London, 2022b). The Mayor of London implemented this ULEZ in a bid to reduce congestion, improve ambient air quality and tackle climate change within London (Transport for London, 2022a). Emissions of NO_X and $PM_{2.5}$ were estimated to have fallen by 35 % and 15 % respectively following 10 months of ULEZ operation compared to a "no ULEZ" scenario (Greater London Authority, 2020). Similarly Hajmohammadi & Heydecker (Hajmohammadi and Heydecker, 2022) identified a 20 % reduction in NO_x concentrations within the ULEZ itself in the 11 months following its introduction in 2019 compared to the preceding 12 months. Conversely, Ma et al. (Ma et al., 2021) reported an average reduction in roadside NO_2 concentrations of less than 3 % throughout the nine months following the ULEZ introduction.

LEZs have been shown to effectively reduce ambient NO_x and PM concentrations (Boogaard et al., 2012; Gómez-Losada and Pires, 2024; Park and Lim, 2025; Poulhès and Proulhac, 2021; Santos et al., 2019), with research indicating that low emission zones (LEZs) are more effective where restrictions apply to cars and light vehicles alongside heavy vehicles compared to those that restrict heavy vehicles alone (Holman et al., 2015; Poulhès and Proulhac, 2021). After five years of operation, the London LEZ, placing restrictions on heavy vehicles alone, was found to have coincided with a 2.5–3.0 % reduction in particulate matter concentrations with no impact on NO_x concentration (Ellison et al., 2013). In contrast, Zone 1 of the Lisbon, Portugal, LEZ placed restrictions on all vehicle types, and saw 29 % and 12 % reductions in PM_{10} and NO_2 respectively (Santos et al., 2019).

Changes in tropospheric trace composition as a result of COVID-19 restrictions across the planet have been widely documented (Cavallaro and Nocera, 2024; Marinello et al., 2021), with studies exploring conditions, for example, within the UK (Jephcote et al., 2021; Skirienė and Stasiškienė, 2021; Vega et al., 2021; Wyche et al., 2021), Iran (Shami et al., 2022), Spain (Ródenas et al., 2022; Skirienė and Stasiškienė, 2021), Mexico (Vega et al., 2021), India (Vega et al., 2021), Italy (Conte et al., 2023), and China (Feng et al., 2021; Xin et al., 2021). Addas & Maghrabi (Addas and Maghrabi, 2021) identified 237 studies assessing the impact of COVID-19 restrictions on air quality, the majority having been conducted within Asia (~65 %) and Europe (~18 %).

Changes in particulate matter mass concentrations during the pandemic were slightly more varied and complex, with the different sizes of particles seeing different changes across different locations as a consequence of COVID-19 restrictions. For example, Wyche et al. (Wyche et al., 2021) found that $PM_{2.5}$ concentrations were ~6 % higher in the southeast of the UK during the initial national lockdown compared to a baseline average taken from the same period throughout 2015–2019, whilst PM_{10} concentrations were ~14 % lower. Conversely, Vega et al. (Vega et al., 2021) reported that $PM_{2.5}$ concentrations reduced by 25 % in London between January and August 2020 compared to the same period between 2017 and 2019, again demonstrating that changes in pollutant abundance at the time were not spatially uniform. It is worth noting here that transboundary transport likely played an important role in determining overall local PM levels at these sites, for instance back trajectory analyses indicated that air masses brought to the southeast of the UK throughout April 2019 typically originated from the northwest European air pollution "hotspot" region (Munir et al., 2021; Wyche et al., 2021).

Airborne particulate matter has historically been monitored using mass concentration as the measurand, however it has been widely observed that particle number concentration provides a better understanding of risks to human health. Measuring particulates by mass works well in identifying the atmospheric loading of larger PM_{10} and $PM_{2.5}$, particles, however it is now accepted that much smaller, so-called ultrafine particles (UFP), which have negligible mass, should be monitored rather as a number concentration (De Jesus et al., 2019; Hofman et al., 2016; Kwon et al., 2020). UFPs are defined as airborne particles with a diameter $\leq$100 nm (Hong and Jee, 2020), and while larger particles comprise the majority of total PM mass in the atmosphere, UFPs dominate atmospheric particle number density and surface area (De Jesus et al., 2019; Morawska et al., 1999; Vu et al., 2015).

New particles can be emitted directly to the atmosphere via primary routes, including combustion, industrial activity and vehicle usage, or they can be formed *in-situ* via secondary processes, including hydrogen bonding and dipole interactions between gas-phase molecules with a diameter of less than 1 nm, i.e. new particle formation (NPF) (Peng et al., 2023). Consequently, NPF events are closely linked to the abundance of condensable chemical vapours within the atmosphere (Bousiotis et al., 2021; Lee et al., 2019; Zhang et al., 2012), which themselves can be primary or secondary in nature, with the latter being formed via photooxidation of other reactive trace gases (Lee et al., 2019; Zhang et al., 2012). Such important condensable species include sulphuric acid (Guo et al., 2020; Peng et al., 2023), ammonia, amines, and VOCs.

UFPs can be formed in the atmosphere via homogeneous nucleation involving low volatility, condensable gas-phase species (Hao et al., 2015; Holmes, 2007; Zhang et al., 2012). Newly formed particles occupy the nucleation size mode (d $\leq$ 10–25 nm) and their presence and abundance are determined by tropospheric conditions at their time of production, i.e. the number of pre-existing particles in the atmosphere and amount of photochemistry can both affect the rate of production and the half-life of newly formed particles (Guo et al., 2020). UFPs typically possess an atmospheric half-life of the order minutes to hours, which is somewhat shorter than the typical half-life of $PM_{2.5,}$ which tends to be of the order days to weeks (Air Quality Expert Group, 2005; Araujo and Nel, 2009). Nucleation mode particles exist in the air for a relatively short period of time (ca. < 1 h) before growing into larger Aitken mode particles (d 25 $\leq$ 100 nm) (Spurny, 1998), with accumulation mode particles (d $\geq$ 100 nm) typically remaining extant for as long as 7–30 days (Kwon et al., 2020).

This paper assesses the impact of ULEZ and COVID-19 restrictions on ambient atmospheric composition in Marylebone, London, UK, focussing predominantly on changes in Ultrafine Particulate (UFP) size distribution and number concentration utilising data collected between January 2015 and December 2022, utilising Gradient Boosted Regression models to remove variations attributable to meteorological conditions.

2. Methodology

2.1. Marylebone Road AURN monitoring station

The Marylebone Road Automatic Urban and Rural Network (AURN) monitoring station is an Urban Traffic site located within a street canyon in central London, UK, approximately 1 m from the regularly congested six-lane A501 road (Department for Environment, 2022). The A501 forms the northern boundary of the London Congestion Charge Zone, and the site is situated within the boundaries of the London ULEZ (Transport for London, 2022b). The Marylebone Road AURN station is highly instrumented with numerous monitors, including a NO_x chemiluminescence analyser and O_3 UV absorption analyser (Department for Environment and Food and Rural Affairs, 2024); a Condensing Particle Counter (CPC, TSI 3772); and a Scanning Mobility Particle Sizer (SMPS;

TSI 3936) consisting of a CPC (TSI 3775) and an electrostatic classifier (TSI 3080) which further consisted of a Kr-85 charge neutraliser (70 MBq and a Differential Mobility Analyser (DMA; TSI 3081) (Ciupek et al., 2023). This SMPS has a PM_1 cut off in place until August 2022, at which point it was replaced by a $PM_{2.5}$ cut off. A Nafion drier system was in place throughout the study period, maintaining a relative humidity of less than 40 %. No correction was made for diffusion losses within the inlet system, however corrections were made for internal losses within the instruments.

For this study, NO_2, O_3, $PM_{2.5}$ and PM_{10} measurements came from UK AURN measurement available using the "openair" R package (Carslaw and Ropkins, 2022). Data between January 2015 and December 2022, alongside particle number concentrations within fifty-one different size channels over the range 15.92–625.25 nm between January 2016 and October 2022 where used in the analysis. The particle number concentration was converted to $dN/dlogD_p$ values using the "foqat" R package (Chen, 2023). These data were supplemented with a) modelled wind speed, wind direction and temperature values for Marylebone Road, b) relative humidity observations made at St James's Park (~3.6 km southeast of Marylebone Road), sourced from NOAA's Integrated Surface Database (NOAA-ISD) using the "worldmet" R package (Carslaw, 2023a), c) hourly MIDAS Open rainfall (Met Office, 2023a) and solar radiation (Met Office, 2023b) observations made at Kew Gardens, and d) hourly traffic count data for Marylebone Road supplied by Transport for London (Transport for London, 2021; Transport for London, 2023). Hour, day of week, week number and month were extracted from the data and used as independent variables for modelling.

2.2. Model production

All datasets were screened for anomalies, errors, maintenance periods or equipment failure, with observations deleted where issues were identified. Model production was undertaken using R [v4.3.1 (R Core Team, 2024)]. To establish changes as a result of these interventions, the observed data was "deweathered" to account for the influence of meteorological factors. To account for the meteorological variation, the "deweather" package (Carslaw, 2023b), based upon boosted regression trees via the "gbm" package (Ridgeway, 2024), was utilised to a) assess the appropriate number of trees and overall model effectiveness, b) produce boosted regression tree models for all air pollutants using temporal and meteorological variables (overall trend, hour of day, day of week, week of year, month of year, wind direction, wind speed, traffic count, relative humidity, air temperature, solar radiation and precipitation) as predictors, c) assess the influence of predictor variables on air pollutants, and d) predict air pollutant concentration 200 times using a random sample of meteorological conditions. This approach enables an assessment of pollutant abundance and trends in the absence of outside influences. The use of 1500 trees represented a balance between over/under-fitting for all air pollutants, and this value was used in the production of all deweather models. Using the "metSim" function in the "deweather" package, the BRT models were used to predict pollutant concentration 200 times, with the columns containing the twelve predictor variables, excluding overall trend, uniquely shuffled for each prediction round. These predictions were then averaged into a single returned timeseries, with this representing the predicted concentration without the variation introduced by the predictor variables, i.e. the "deweathered" concentration.

A similar methodology was used by Ceballos-Santos et al. (Ceballos-Santos et al., 2021) to assess air pollutant concentrations in northern Spain. Boosted regression tree models are produced by combining a large number of comparatively simple decision tree models, which themselves are resistant to outliers and gaps within predictor variables, as well as automatically assessing interactions between predictor variables (Elith et al., 2008). Once produced, the decision tree models are iteratively fitted to the training data, emphasising cases poorly predicted by previously fitted through re-weighting (Carslaw and Taylor, 2009; Elith et al., 2008; Leathwick et al., 2006).

2.3. Data analysis

The model partial dependencies were assessed using the "deweather" package to determine the influence of independent variables on air pollutant concentrations. The "openair" package [v2.18-0; 48] was used to produce Theil-Sen trend analyses and time variation plots for all air pollutants. Time variation analyses were undertaken for each of the 51 UFP channels, with the daily average concentration for each period/channel extracted to allow an investigation into absolute and percent change.

To assess the changes in the abundance of nucleation, Aitken and accumulation mode UFP following the implementation of ULEZ and COVID-19 measures, kernel density estimation plots were generated for each of the three periods. Additionally, a Theil-Sen trend analysis of the percentage of UFP TNC comprised of nucleation mode particles was undertaken to assess long term changes in particle size distribution.

3. Results and discussion

3.1. Influence of predictor variables

Meteorological conditions typically exhibit a greater influence on ambient atmospheric composition than an intervention event (Anh et al., 1997), with assessments of the impact of an intervention complicated by the ever-changing nature of meteorological conditions (Grange and Carslaw, 2019). To assess the overall influence of each predictor variable on trace gas and aerosol abundance, the partial dependencies of the Gradient Boosted Regression models were assessed. The overall influence is given as a percentage in Table 1, with plots available in the SI. Wind direction had the highest influence on both Aitken (22.6 %) and nucleation (34.0 %) mode particles and the second highest influence on accumulation mode particles (11.9 %). Traffic count accounted for 17.2 % and 10.8 % of the variation in Aitken (2nd of 12) and nucleation (3rd of 12) abundance respectively, with higher traffic volumes associated with higher concentrations of both particle modes. Wind speed had a relatively large influence on concentrations of both accumulation (10.6 %, 3rd of 12) and Aitken (11.8, 4th of 12) mode particles, with abundance decreasing as wind speed increased, whilst showing a notably reduced influence on nucleation mode particle abundance (5.2 %, 7th of 12). The predictor analysis shows the strong dependency of UFP on traffic sources [e.g. (Hama et al., 2017)].

Predictor variables had similar influences on both $PM_{2.5}$ and PM_{10}, with overall trend and wind direction having the most influence on PM concentration indicative of transport influences (Air Quality Expert Group, 2005). Month and wind speed had the third and fourth largest

Table 1
The percentage of variation within trace gases and aerosols attributed to each of the 12 predictor variables, with the three largest influences differentiated in bold (see also Fig. A2 to A8). Acc. = Accumulation mode UFP, Nuc. = Nucleation mode UFP.

Predictor Variable	NO_2	O_3	PM_{10}	$PM_{2.5}$	Acc.	Aitken	Nuc.
Trend	***22.6***	***17.0***	***26***	***30.4***	***33.4***	***15.3***	***17.5***
Hour of day	*8.7*	*2.3*	*4.5*	*3.6*	*3.9*	*7.0*	*6.0*
Day of week	*4.4*	*3.2*	*5.0*	*4.5*	*4.9*	*4.8*	*4.8*
Week of year	*0.8*	*1.1*	*4.4*	*3.4*	*3.1*	*2.3*	*2.1*
Month of year	*3.1*	*14.4*	***12.4***	*11.8*	*6.1*	*6.0*	*6.3*
Wind Speed	*3.8*	*9.5*	*12.0*	***13.4***	***10.6***	*11.8*	*5.2*
Wind Direction	***22.8***	***18.2***	***15.6***	***14.3***	***11.9***	***22.6***	***34.0***
Temperature	*3.9*	*2.8*	*4.5*	*5.4*	*6.6*	*4.0*	*4.1*
Relative Humidity	*2.1*	***20.7***	*5.1*	*6.4*	*8.0*	*6.6*	*5.8*
Solar Radiation	*1.7*	*1.5*	*1.8*	*1.1*	*1.4*	*2.2*	*3.1*
Precipitation	*0.1*	*0.2*	*1.5*	*1.0*	*0.3*	*0.3*	*0.4*
Traffic Count	***26.0***	*9.1*	*7.0*	*4.7*	*9.5*	***17.2***	***10.8***

influence on PM_{10} concentration, reversed to the fourth and third respectively for $PM_{2.5}$. All predictor variables largely had the same influence on both PM_{10} and $PM_{2.5}$, with the most notable difference being that peak in $PM_{2.5}$ concentrations typically lagged those of PM_{10} by around 2 h.

The NO_2 partial dependencies show the predominant influences on variations in NO_2 concentrations were traffic count, wind direction and the overall trend, with relative humidity having little influence upon this variation indicative of the strong traffic source term. Contrastingly, relative humidity, wind direction and overall trend were the three predominant factors driving variations in O_3 abundance, with traffic count having a notably lower overall influence (9.1 %). Wind speed had a higher influence on O_3 compared to NO_2; it is however notable that this influence was reversed, with higher wind speeds aligned with higher O_3 and lower NO_2 concentrations. This reversal was also shown within the more influential wind direction, with southerly and northerly winds aligned with higher NO_2 and O_3 concentrations, respectively. The diurnal relationship between the two pollutants is observable when assessing the influence of time of day (hour) and month of year (month).

Whilst vehicle movements gradually reduced between January 2015 and February 2020, the average number of vehicle movements per hour ranged from ~2600 (March 2018) to ~3500 (October 2015) (see Fig. A9). The implementation of COVID-19 restrictions was characterised by a sudden and rapid reduction in hourly vehicle movements, falling from 2994 to 1340 between February and April 2020. Traffic volumes increased sharply to 2218 in June 2020, typically continuing to increase gradually throughout the remainder of the study period. Exceptions were identified in November 2020 and early 2021, again aligning with the introduction of COVID-19 restrictions.

3.2. UFP size distribution

Particulate matter exhibits a multi-lognormal distribution that is typically considered to be comprised of four modes i.e. the nucleation, Aitken, accumulation, and coarse modes (Vu et al., 2015; von Bismarck-Osten et al., 2013; Kulmala et al., 2017). When the quadmodal distribution is utilised, nucleation mode typically comprises particles less than 20 nm (Kulmala et al., 2017; Wu et al., 2008), 25 nm (Komppula et al., 2003) or 30 nm (Vu et al., 2015; von Bismarck-Osten et al., 2013), with Aitken mode particles spanning from the upper nucleation mode limit to 90 nm (Kulmala et al., 2017), 95 nm (Komppula et al., 2003) or 100 nm (Vu et al., 2015; von Bismarck-Osten et al., 2013; Wu et al., 2008). The accumulation mode includes all suspended particles between the upper Aitken limit and 500 nm (Komppula et al., 2003) or 1000 nm (Vu et al., 2015; Wu et al., 2008), with von Bismarck-Osten et al. (von Bismarck-Osten et al., 2013) providing no upper boundary for the accumulation mode. All particulates larger than the upper boundary of the accumulation mode are classified as belonging to the coarse mode.

Nucleation mode particles were defined as those with a diameter less than 25 nm, with Aitken comprising those with a diameter between 25 and 100 nm. Those particles larger than 100 nm were defined as accumulation mode. As shown in Fig. 1, the mean daily concentration of all particles with a diameter of 19.85 nm or less increased following the introduction of the ULEZ and the onset of the COVID-19 restrictions. More specifically, the absolute concentrations of particles measured in

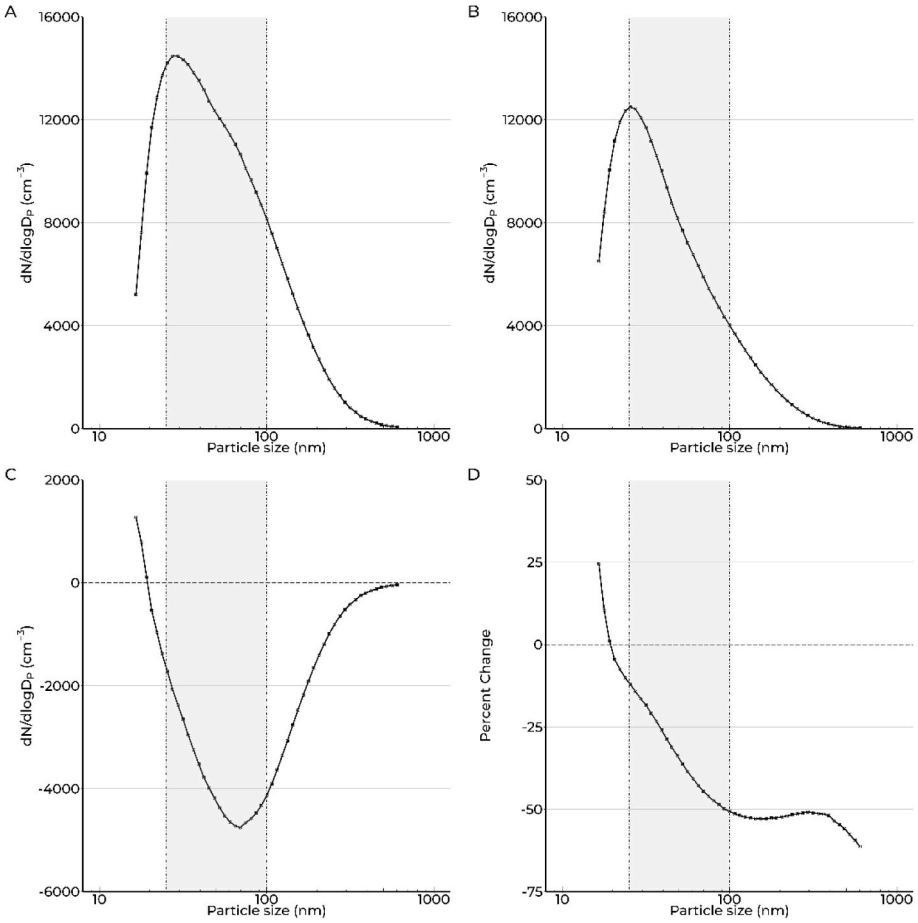

Fig. 1. UFP size distribution before (A) and after (B) ULEZ introduction represented in dN/dlogDp, with the change in particle-size distribution following ULEZ introduction (2019–2022) compared to pre-ULEZ (2015–2019) both in dN/dlogDp (C) and as a percentage change (D). Vertical lines mark the Nucleation/Aitken and Aitken/Accumulation mode boundaries at 25 nm and 100 nm respectively.

the 16.55, 17.80 and 19.15 nm (midpoint) channels were found to have increased by 39.9, 24.7 and 3.5 cm^{-3}, respectively (see Fig. 1C). Conversely, concentrations of all particles with diameters larger than 19.85 nm were found to have reduced over this period, with the largest absolute reduction of 148.6 cm^{-3} being observed in the 69.75 nm (midpoint) channel. As can be seen from inspection of Fig. 1D, the largest relative change in particle number occurred in the 604.3 nm channel, where concentrations were found to have reduced by 61.3 %, a consequence of the typically low concentrations of particles of this size observed throughout the study. The 16.55 nm channel exhibited the largest percentage increase in particle number during the study period, i.e. 24.4 %, and the largest absolute increase, i.e. 39.9 cm^{-3}.

Kernel density estimation plots were generated to assess the distribution and variability of nucleation, Aitken and accumulation mode particle abundance before ULEZ introduction (Fig. 2A), during ULEZ restrictions alone (Fig. 2B) and during both COVID-19 and ULEZ restrictions (Fig. 2C). Throughout the study period, the number concentration of Aitken mode particles showed a markedly higher range of 5033 (4321–9355 cm^{-3}) compared to the 5033 (751–4036 cm^{-3}) and 2390 (817–3207 cm^{-3}) of accumulation and nucleation mode particles respectively. The mean number concentration of Aitken and accumulation mode particles was 6.6 % and 36.4 % lower respectively under ULEZ restrictions compared to before ULEZ implementation, whilst the mean concentration of nucleation mode particles rose 30.1 %. When COVID-19 restrictions were superimposed onto ULEZ restrictions, mean concentrations of Aitken and accumulation mode particles were 16.9 % and 42.9 % lower than before ULEZ introduction, whilst the mean concentration of nucleation mode particles was 16.3 % higher. This suggests that nucleation mode particles had a higher baseline abundance following the ULEZ and COVID-19 interventions, with coinciding reductions to the baseline abundance of both Aitken and accumulation mode particles.

As per Fig. 3, the percentage of ultrafine particle total number count (UFP-TNC) comprised of nucleation mode particles typically increased by 1.7 % per year ($p < 0.001$, 95 % CI [1.39, 2.09]). This finding aligns with that of Damayanti et al. (Damayanti et al., 2023) observed that the proportion of UFP-TNC comprised of nucleation mode particles rose from 23 % to 39 % between 2015 and 2021, defining nucleation mode particles as having a diameter ≤30 nm. This trend was disrupted from early 2021 until mid 2022, with a 29.6 % reduction in nucleation mode

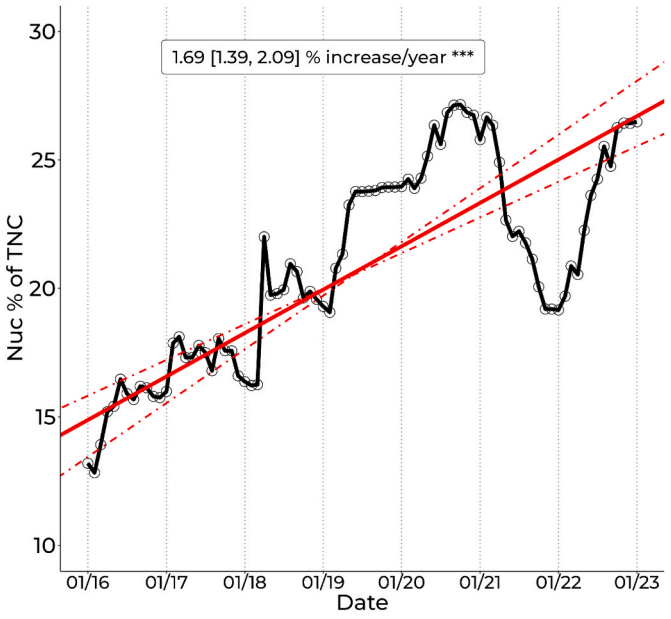

Fig. 3. Theil Sen trend analysis of the proportion of UFP-TNC comprised of nucleation mode particles.

abundance between January 2021 and January 2022 coinciding with an 11.1 % increase in accumulation mode abundance, 2.1 % increase in Aitken mode abundance and a 5.1 % reduction in UFP-TNC abundance. Concentrations of PM_{10} and $PM_{2.5}$ were elevated throughout late 2020 and early 2021. No reasoning for this disruption could be identified within the predictor variables utilised in this study. The apparent growth in NMP could be attributed to a number of different factors including emission changes, change in new particle formation rates or nucleation events as well as scavenging reduction.

3.3. Long-term trends

Theil-Sen trend analysis shows that deweathered and measured NO_2 concentrations at Marylebone Road fell by 7.0 and 7.9 μgm^{-3} per year,

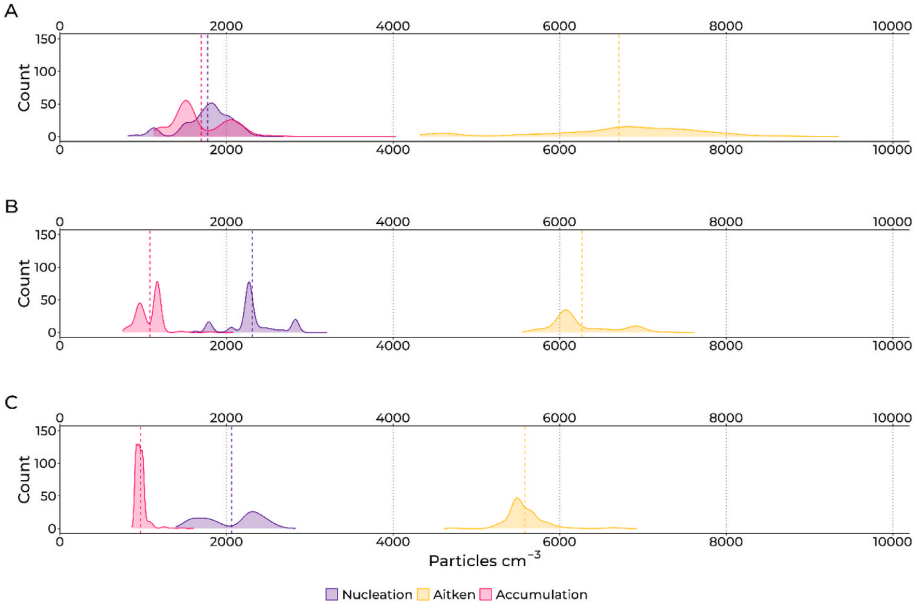

Fig. 2. Kernel density plot of nucleation, Aitken and accumulation mode UFP before ULEZ implementation (A), during ULEZ restrictions alone (B) and during both ULEZ and COVID-19 restrictions (C).

respectively during the study period. Deweathered PM_{10} and $PM_{2.5}$ concentrations fell by 1.1 and 0.8 μgm^{-3} per year, respectively, with measured concentrations falling by 1.3 and 0.9 μgm^{-3}. Number concentrations of both deweathered and measured accumulation mode particles also decreased between 2015 and 2023, by 166.3 and 213.2 cm^{-3} per year, respectively. Similarly, deweathered and measured concentrations of Aitken mode particles fell by 256.0 and 433.2 cm^{-3} per year. In contrast, the deweathered and measured O_3 concentrations increased by 1.9 and 2.0 μgm^{-3} per year, respectively, and deweathered nucleation mode particle number concentrations increased by 122.8 cm^{-3} per year (see Fig. 4). The trend observed in measure NMP number concentration was not statistically significant ($p > 0.05$). These are results similar to those shown by Kamara & Harrison (Kamara and Harrison, 2021), and loosely align with the findings of Damayanti et al. (Damayanti et al., 2023).

To further assess changes in particulate concentration and size distribution, the observed dataset was split into three periods, i.e. "Pre ULEZ", which was defined as January 01, 2015 to April 08, 2019, "ULEZ", defined as April 08, 2019 to March 26, 2020 and February 21, 2022 to December 31, 2022, and "ULEZ & COVID", which was defined as March 26, 2020 to February 21, 2022, the latter group aligning with the introduction and removal of COVID-19 restrictions (Institute for Government, 2022; Sherrington, 2022; The Week, 2020). Time variation plots of PM_{10} (Fig. A10) and $PM_{2.5}$ (Fig. A11) show their respective

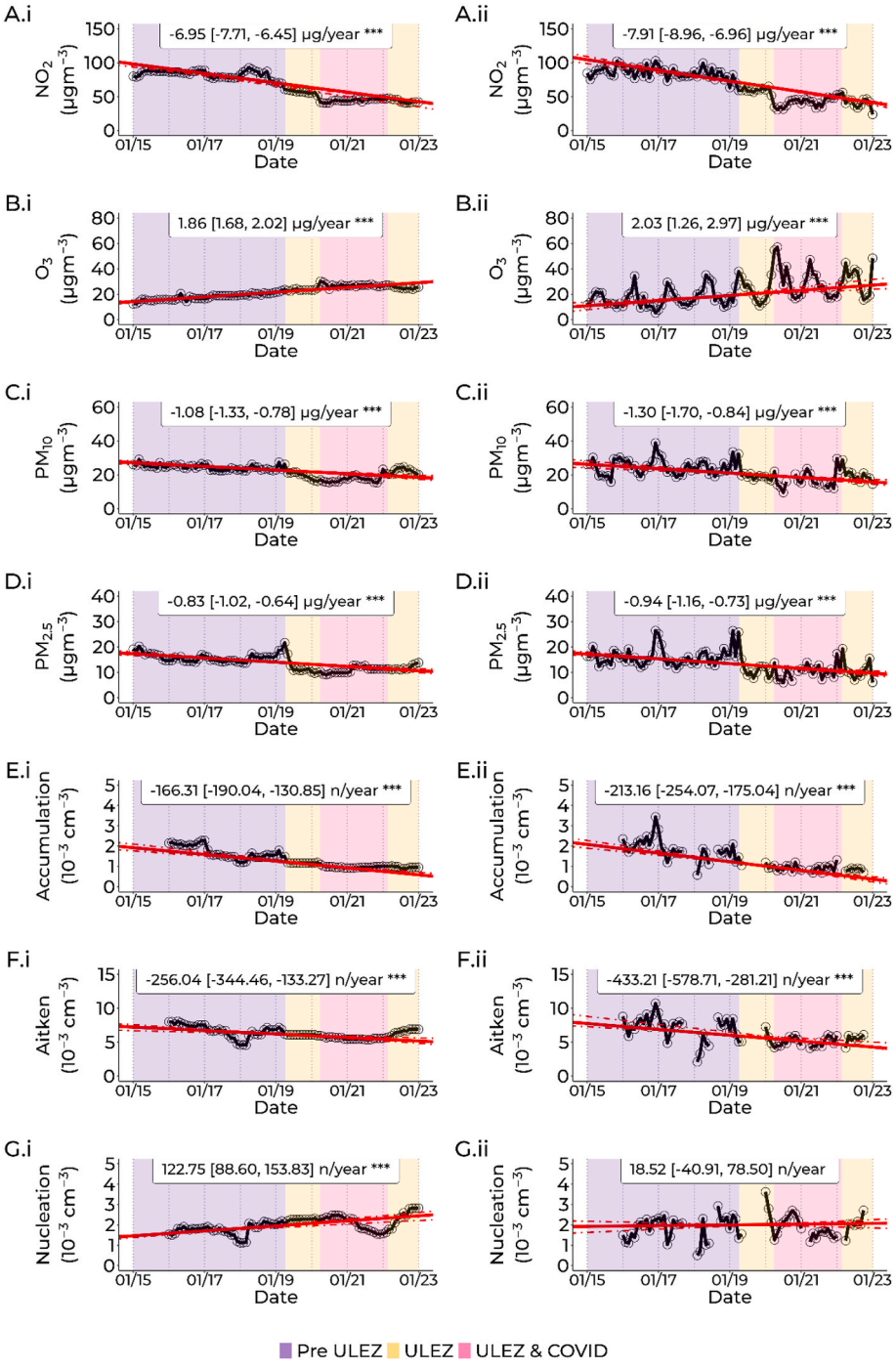

Fig. 4. Theil-Sen trend analyses for deweathered (.i) and observed (.ii) NO_2 (A), O_3 (B), PM_{10} (C), and $PM_{2.5}$ (D), with accumulation (E), Aitken (F), and nucleation (G) mode UFP ($p < 0.001$ = ***, $p < 0.01$ = **, $p < 0.05$ = *, $p > 0.05$ is blank).

concentrations were lower at all times of the day, week and year except April following ULEZ introduction, with mean hourly concentrations of both measurands falling by 4.6 μgm^{-3}. When COVID-19 restrictions were imposed on top of ULEZ restrictions, mean concentrations of PM_{10} and $PM_{2.5}$ fell an additional 2.8 and 1.3 μgm^{-3} compared to abundance during ULEZ restrictions alone.

Time variation plots were produced for nucleation, Aitken and accumulation mode particles to assess temporal variations in particle abundance throughout the three defined periods (Figs. 5 and 6). Typical accumulation and Aitken mode particle abundance were consistently higher before the introduction of the ULEZ, exhibiting a bimodal daily pattern. Throughout all periods, concentrations of both particle modes peaked ain the late evening at ~9pm, reducing overnight into the early morning at ~4am, sharply increasing throughout the morning rush hour. A second sharp increase is apparent from late afternoon from ~4pm until the late evening, with this more apparent in Aitken mode particles. The typical early morning (4am) concentration of accumulation and Aitken mode particles was 40.2 % and 13.6 % lower under ULEZ restrictions alone compared to before ULEZ introduction. Prior to ULEZ introduction, typical accumulation and Aitken concentrations at 9am were respectively 70.3 % and 99.1 % higher than those at 4am, compared to increases of 29.8 % and 47.9 % during ULEZ operation. Under both ULEZ and COVID-19 restrictions, concentrations of accumulation and Aitken modes increased by 15.4 % and 54.3 % between 4am and 9am.

Variations in concentrations of nucleation mode particles exhibited a rough bimodal pattern, with concentrations generally peaking in both the morning and evening (Fig. 7). Morning concentrations typically peaked at 9am prior to ULEZ implementation after rising steadily since ~4am, however under ULEZ operation, both during and outside of COVID-19 restrictions, this peak typically instead occurred at 6am. Under ULEZ alone, concentrations at 6am were typically 21.0 % higher than at the same time before ULEZ introduction, compared to 11.8 % lower at 9am. Notably, concentrations of nucleation mode particles generally decreased between 9am and 4pm prior to ULEZ introduction before increasing throughout the evening rush hour. In contrast, concentrations began to increase in the late morning during ULEZ both with and without COVID-19. Concentrations were typically higher throughout the week following ULEZ implementation than before, with the exception of Thursday and Friday, whilst concentrations generally reduced at all times during COVID-19 restrictions.

These observations suggests that a potential change in tropospheric composition or conditions was brought about by the introduction of the ULEZ, which suppressed ambient levels of PM_{10}, $PM_{2.5}$, accumulation and Aitken mode particles. The reduction in particle abundance throughout overnight is indicative of a reduction in anthropogenic emissions throughout these hours coupled to boundary layer dynamics. Wehner et al. (2009) found that emissions of both nucleation (<25 nm) and "soot" (25–400 nm) particles from diesel engines were typically 10 and 100 times higher than from gasoline (petrol) engines in urban traffic environments, which suggests the changes seen following ULEZ implementation are a result of a reduction the number of in older, predominantly diesel fuelled vehicles entering central London.

3.4. Impacts of interventions

3.4.1. ULEZ

Inspection of Fig. 4 also shows that to various degrees, the pollutants investigated here also underwent more abrupt, step-like changes in concentration at certain times between 2016 and 2023, including in 2019 when the ULEZ was introduced and in 2020 when COVID-19 restrictions came into force. For instance, between March and April of 2019 as the ULEZ came on-line, analysis shows that mean monthly deweathered NO_2 concentrations (Fig. 4a i) fell sharply by 8.6 μgm^{-3} (−12.4 %) i.e. 124 % of the annual reduction predicted by the Theil-Sen trend analysis, and that deweathered O_3 concentrations (Fig. 4b i) increased by 0.7 μgm^{-3} (+3.2 %), i.e. 39 % of the average annual rise.

Deweathered concentrations of PM_{10} (Fig. 4c i) and $PM_{2.5}$ (Fig. 4d i) increased between March and April 2019 immediately following ULEZ introduction, by 2.8 μgm^{-3} (+12.1 %) and 3.0 μgm^{-3} (+15.8 %) respectively. Deweathered $PM_{2.5}$ abundance then decreased by 10.9 μgm^{-3} (−50.2 %) between April and July 2019 before reaching a plateau. Deweathered PM_{10} abundance decreased by 5.0 μgm^{-3} (−19.0 %) between April and May 2019, plateaued from May to August 2019 (−5.3 %), and then decreased sharply through to February 2020, where it reached a value of 16.5 μgm^{-3} (−18.1 %). Between March and December 2019, deweathered PM_{10} abundance had declined by 4.8 μgm^{-3} (449 % of the typical annual change), and deweathered $PM_{2.5}$ abundance had reduced by 7.2 μgm^{-3} (877 % of the typical annual change).

Whilst the ULEZ was introduced in April 2019, deweathered accumulation and Aitken mode number concentrations exhibited a decline between February and June 2019, with their respective concentrations falling by 616.7 cm^{-3} (from 1787.6 to 1170.9 cm^{-3}) i.e. 370.9 % of the average annual reduction (Fig. 4e i) and 1096.8 cm^{-3} (from 7172.7 to 6075.9 cm^{-3}) i.e. 428.4 % of the average annual reduction (Fig. 4f i). Conversely, nucleation mode number concentrations were found to have increased between January and June 2019, with concentrations going

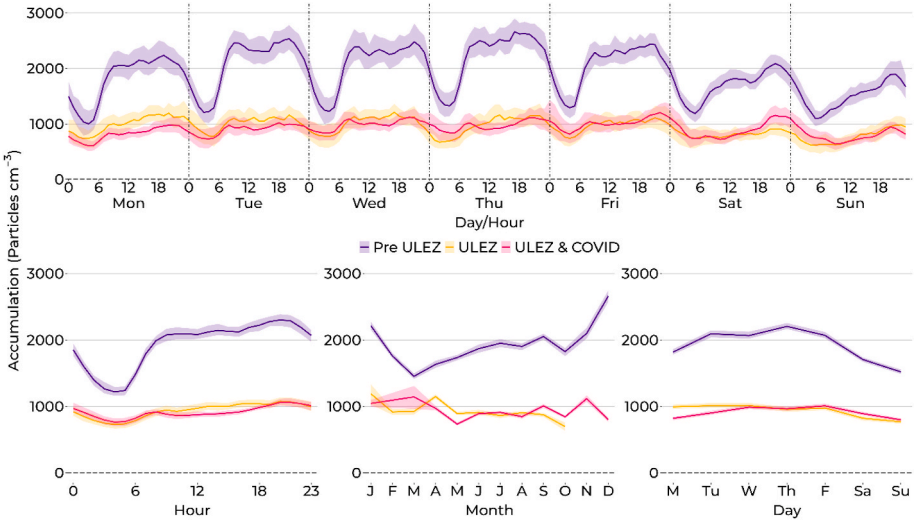

Fig. 5. Time variation plot of accumulation mode particle abundance.

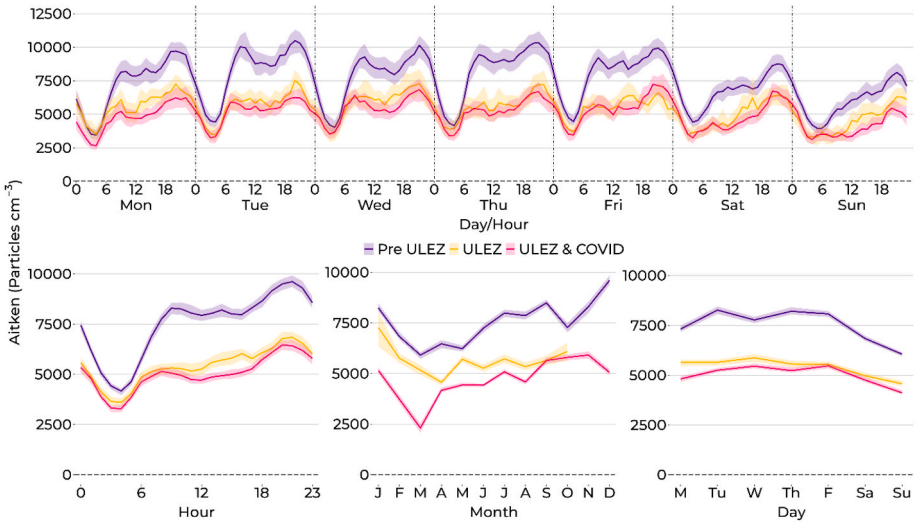

Fig. 6. Time variation plot of Aitken mode particle abundance.

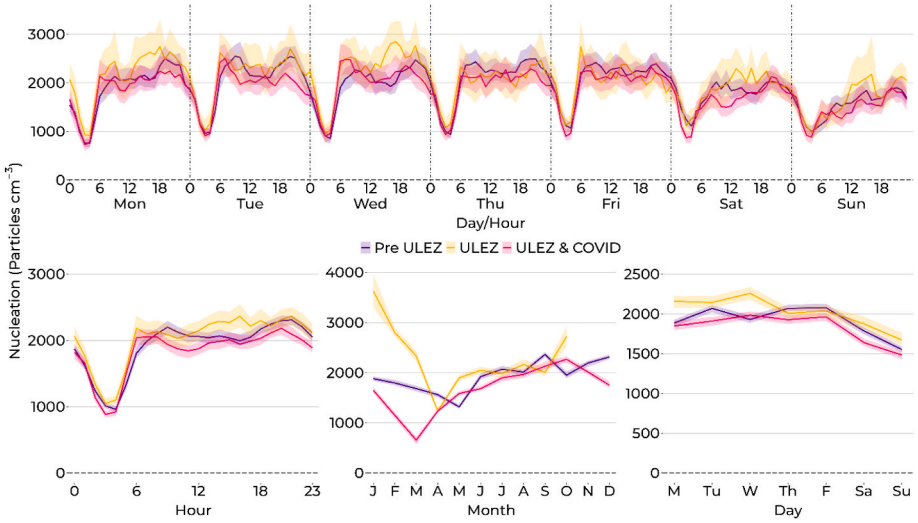

Fig. 7. Time variation plot of nucleation mode particle abundance.

up by 150.7 cm^{-3} (from 2109.0 to 2259.8 cm^{-3}), i.e. 122.8 % of the average annual increase (Fig. 4g i).

It is clear from the analysis that ULEZ implementation did expedite reductions in the abundance of NO_2, PM_{10}, $PM_{2.5}$, accumulation and Aitken mode particles at this heavily trafficked site, as can be clearly seen by the step changes present within the Theil-Sen analyses. However, these reductions did coincide with concomitant increases in ambient O_3 and nucleation mode particle abundance. It is reasonable to suggest that these changes are linked to one another, with this study observing an increase in nucleation mode particle abundance aligning with reductions in both Aitken and accumulation mode particle and PM abundance, supporting the current understanding that in polluted environments, newly formed particles are typically scavenged rapidly by larger, pre-existing PM (Guo et al., 2020; Kulmala et al., 2017; Xiao et al., 2021) and that newly formed particles generally show a higher growth rate in polluted or urban areas compared to cleaner or rural areas (Hao et al., 2015).

3.4.2. COVID-19

During the March to June 2020 lockdown period, mean NO_2, PM_{10} and $PM_{2.5}$ concentrations were 45.7 %, 33.2 % and 41.0 % lower than their respective mean concentrations throughout the same period of 2015–2019, with mean O_3 concentration 49.0 % higher than the baseline through this period (Table 2). Between February and April 2020, mean monthly deweathered NO_2 concentrations at Marylebone Road fell by 15.0 μgm^{-3} (−26.4 %), i.e. 215.7 % of the average annual reduction. Through the same period, O_3 concentrations increased by 6.8 μgm^{-3} (+28.8 %), i.e. 362.0 % of the average annual increase, with PM_{10} and $PM_{2.5}$ abundance increasing by 0.6 μgm^{-3} (+3.5 %) and 0.7 μgm^{-3} (+6.7 %), respectively. Both PM_{10} and $PM_{2.5}$ abundance then decreased by 1.4 μgm^{-3} (−8.0 %) and 1.2μgm^{-3} (−11.7 %), respectively between April and June 2020. This resulted in a net reduction of 0.8

Table 2
Mean hourly concentration of trace pollutants during March and June 2015–2019 and 2020. Note: * indicates pollutant baseline is 2016–2019.

	Baseline (2015–2019)	2020	% change
NO_2 (μgm^{-3})	80.4	43.7	−45.7
O_3 (μgm^{-3})	18.8	28.0	+49.0
PM_{10} (μgm^{-3})	24.3	16.2	−33.2
$PM_{2.5}$ (μgm^{-3})	16.3	9.6	−41.0
Accumulation* (cm^{-3})	1605.7	1072.9	−33.2
Aitken* (cm^{-3})	6663.3	5857.0	−12.1
Nucleation* (cm^{-3})	1877.8	2295.7	+22.3

μgm^{-3} in PM_{10} and 0.6 μgm^{-3} in $PM_{2.5}$ abundance, i.e. 73.3 % and 66.1 % of the respective average annual reductions between February and June 2020.

Similarly, accumulation and Aitken mode concentrations were 33.2 % and 12.6 % lower respectively between March and June 2020 than the same period throughout 2016–2019, with nucleation mode concentration being 22.3 % higher than the baseline period (Table 2). Through the same period, accumulation and Aitken mode abundance respectively increased by 209.2 cm^{-3}, i.e. 125.8 % of the average annual reduction, and 312.3 cm^{-3}, i.e. 122.0 % of the average annual reduction, with nucleation mode abundance increasing by 127.3 cm^{-3}, i.e. 103.7 % of the average annual reduction.

Existing research has shown that NO_x concentrations fell across all inhabited continents during the various stages of the COVID-19 pandemic, however concentration reductions were not spatially uniform (Addas and Maghrabi, 2021). During the initial phase of COVID-19 restrictions, ambient NO_2 concentrations were found to have fallen by between 12 % (rural background) and 38 % (kerbside) within southeast England (Wyche et al., 2021), and 40 % within London (Potts et al., 2021; Vega et al., 2021). In addition, both Ropkins & Tate (Ropkins and Tate, 2021) and Jephcote et al. (Jephcote et al., 2021) found that average NO_2 concentrations at roadside monitoring stations specifically had declined by 32 % and 47.9 % respectively, whilst Lee et al. (2020) reported an average NO_2 reduction of 42 % (±9.8 %) across the country. Conversely, O_3 concentrations were found to have generally increased. In studies focussed on the UK, Wyche et al. (Wyche et al., 2021), Ropkins & Tate (Ropkins and Tate, 2021) and Lee et al. (Lee et al., 2020) reported average increases in O_3 abundance of 6 %, 14 % and 11 % at urban background sites within their respective areas of research, with Jephcote et al. (Jephcote et al., 2021) identifying an average 34.1 % increase in O_3 concentrations at roadside monitoring locations within London.

This reflects a general trend that was observed across the world, with Marinello et al. (Marinello et al., 2021) stating that studies had reported an average increase of 47 % in O_3 concentrations during the pandemic. Such increases were not seen uniformly, with Vega et al. (Vega et al., 2021) finding O_3 concentrations had reduced by 24 % in Delhi (India), 6 % in Mexico City (Mexico), and 33 % in London (UK). However Marinello et al. (Marinello et al., 2021) highlighted that O_3 is the trace gas that is most commonly reported to have become more abundant throughout the COVID-19 response. This finding is likely a result of the different local meteorological conditions across the study sites and whether O_3 concentrations were previously suppressed by either hydrocarbon and/or NO_x (Sillman, 1999).

Changes in particulate matter mass concentrations during the pandemic were slightly more varied and complex, with the different sizes of particles seeing different changes across different locations as a consequence of COVID-19 restrictions. For example, Wyche et al. (Wyche et al., 2021) found that $PM_{2.5}$ concentrations were 6 % higher in the southeast of the UK during the initial national lockdown compared to a baseline average taken from the same period throughout 2015–2019, whilst PM_{10} concentrations were 14 % lower. Comparatively, Vega et al. (Vega et al., 2021) reported that $PM_{2.5}$ concentrations increased by 11 % in London, again demonstrating that changes in pollutant abundance at the time were not spatially uniform. Jephcote et al. (Jephcote et al., 2021) identified a 12.6 % reduction in $PM_{2.5}$ concentrations at urban background locations within London. It is worth noting here that transboundary transport likely played an important role in determining overall local PM levels at these sites, for instance back trajectory analyses indicated that air masses brought to the southeast of the UK throughout April 2019 typically originated from the northwest European air pollution "hotspot" region (Munir et al., 2021; Wyche et al., 2021).

The 26.4 % decrease and 28.2 % increase in deweathered NO_2 and O_3 abundance between February and April 2020 is in keeping with the findings of previous studies investigating UK air at this time. A 6.7 % increase in deweathered $PM_{2.5}$ abundance between February and April 2020 is in keeping with the increase reported by Wyche et al. (2021) and supports the 2.5 % increase observed by Ropkins & Tate (Ropkins and Tate, 2021) at urban traffic locations. The 3.5 % increase in deweathered PM_{10} abundance contrasts with the 14 % reduction observed by Wyche et al. (2021) and Ropkins & Tate (Ropkins and Tate, 2021), respectively. Longer term, the 4.8 % and 5.7 % reductions in deweathered PM_{10} and $PM_{2.5}$ concentrations between February and June 2020 support the conclusions of Vega et al. (2021), in that early 2020 abundance was lower than the average concentrations experienced during early 2017, 2018 and 2019. The findings of this research provide further evidence to support the suggestion of non-uniformity within changes in PM abundance as a consequence of COVID restrictions made by Ropkins & Tate (Ropkins and Tate, 2021).

The relationship between tropospheric NO_x and O_3 has long been established [e.g. Monks et al., 2015], and it is now well known that depending on the NO_x-O_3-hydrocarbon balance, a reduction in NO_x can lead to such an increase in O_3 abundance (Clapp and Jenkin, 2001; Monks et al., 2015; Sillman, 1999; Wyche et al., 2021).

4. Conclusion

Whilst the results of this study are given in the context of existing research, the findings are based solely upon observations made at a single roadside monitoring site in central London. Additionally, this research relies on gradient boosted regression models produced using observed concentrations. No model is 100 % reliable or accurate, although every effort has been made to ensure the resultant models are robust and an accurate depiction of atmospheric composition.

The consequences of changes in tropospheric composition observed in this study are likely to be mixed. It is arguable that lower NO_2 abundance alongside higher O_3 abundance is likely to have negative implications for acute conditions based on short-term exposure, particularly during the warmer, brighter summer months. Such tropospheric conditions may lead to an increase in cardiorespiratory mortality alongside the onset and worsening of respiratory health, including asthma, bronchitis, and COPD, although reductions in the abundance of larger particles may negate this trend to some extent. However, the coinciding increase in nucleation mode abundance is likely to have further consequences with regard to long-term health and mortality, particularly given their ability to translocate within the body. This study emphasises the importance of evaluating the impacts of interventions on all atmospheric pollutants, particularly where reductions in concentrations of targeted pollutants (e.g. NO_X) have the potential to have knock on effects on secondary pollutants (e.g. O_3).

It would be reasonable to suggest NO_X-targeting policies and interventions, along with their associated impacts, define both NO_2 and O_3 as a single pollutant, O_X, or via a two-pollutant model, as described by Williams et al. (Williams et al., 2014). It has long been recognised that tropospheric NO_X and O_3 abundances are intrinsically linked (Leighton, 1961), with rapid interconversion between the two compounds occurring throughout daylight hours (Monks et al., 2015). The harmful effects of both NO_X and O_3 are caused, at least in part, via oxidative stress, thereby having similar impacts upon human health (Lelieveld et al., 2021; Li et al., 2024).

Whilst there is relatively little understanding of the health impacts of long-term exposure to UFPs (Moreno-Ríos et al., 2022), it is recognised that particulate matter has a greater impact on human health as particle size decreases (Brown et al., 2013; Kwon et al., 2020; Oberdörster et al., 2004; Schraufnagel, 2020). However, the World Health Organization (WHO) note that research assessing health implications of UFP exposure are continuing to emerge, with evidence sufficient to allow the production of a "good practice statement" (World Health Organisation, 2021). It has also been widely observed that the use of particle number concentration as the measurand provides greater insight into the risk that PM, including UFP, poses to human health, with the use of particle mass concentration alone preventing the measurement of UFPs within

the atmosphere owing to their negligible mass (De Jesus et al., 2019; Hofman et al., 2016; Kelly and Fussell, 2012; Kwon et al., 2020; Morawska et al., 1999; Vu et al., 2015). The WHO state that it is good practice to measure both ambient UFP number concentration and size-segregated number concentration, with a lower size limit of $\leq$10 nm and no upper bound (World Health Organisation, 2021).

The ULEZ was introduced in April 2019 to improve ambient air quality within Central London by discouraging the use of vehicles which do not comply with specific NO_X and PM emissions standards (Transport for London, 2024). After 10 months of operation, NO_X and $PM_{2.5}$ emissions were estimated to have reduced by 35 % and 15 % respectively compared to a "no ULEZ" scenario (Greater London Authority, 2020), with roadside NO_2 concentrations in 2023 estimated to have been 23 % lower than would have been expected in the "no ULEZ" scenario (Greater London Authority, 2024).

This study has shown that the introduction of the ULEZ did expedite the decline in NO_2, PM_{10}, $PM_{2.5}$ and both accumulation and Aitken mode particle abundance, whilst identifying concomitant increases in O_3 and nucleation mode particle abundance. Existing research suggests that exposure to high concentrations of O_3 are more damaging to human health than an equivalent exposure to NO_2 [e.g. (Crapo et al., 1984; Mustafa et al., 1984; Williams et al., 2014)]. Similarly, it has long been understood that finer particles are typically more deleterious than their larger counterparts [e.g. (Miller et al., 1979)], and thereby smaller, more difficult to measure particles should not be disregarded when assessing the impact of ambient air quality on human health.

The findings of this study indicate that both the implementation of both the ULEZ and COVID-19 restrictions led to reductions in ambient concentrations of larger particles (i.e. PM_{10}, $PM_{2.5}$ and accumulation and Aitken mode particles). Similarly, reductions in NO_X concentrations in turn led to higher concentrations of O_3. Whilst the introduction of the ULEZ has been successful in achieving reductions in NO_2 and $PM_{2.5}$, the outcomes of this study indicate that the wider goal of *improving* air quality is more complicated than achieving reductions in two air pollutants.

CRediT authorship contribution statement

Douglas J. Gregg: Writing – review & editing, Writing – original draft, Visualization, Software, Methodology, Investigation, Formal analysis, Data curation. **Jordan Tompkins:** Writing – review & editing, Data curation. **Rebecca L. Cordell:** Writing – review & editing, Data curation. **Andrew S. Brown:** Writing – review & editing, Data curation. **Kirsty L. Smallbone:** Conceptualization. **Joshua D. Vande Hey:** Writing – review & editing, Supervision. **Kevin P. Wyche:** Writing – review & editing, Supervision, Conceptualization. **Paul S. Monks:** Writing – review & editing, Supervision, Funding acquisition, Conceptualization.

Code availability

The underlying code for this study is available via Mendeley Data (doi: 10.17632/5f8dnmr3zn.1).

Financial support

This research has been supported by NERC CENTA2 grant NE/S007350/1, and NERC grant NE/V009400/1. JVH acknowledges funding from the NIHR Health Protection Research Unit in Chemical Threats and Hazards.

Declaration of competing interest

The authors declare the following financial interests/personal relationships which may be considered as potential competing interests: Paul S Monks reports financial support was provided by UK Research and Innovation Natural Environment Research Council. Joshua Vande-Hey reports financial support was provided by National Institute for Health and Care Research. Other authors declare that they have no known competing financial interests or personal relationships that could have appeared to influence the work reported in this paper.

Acknowledgements

This research used the ALICE High Performance Computing facility at the University of Leicester.

Appendices.

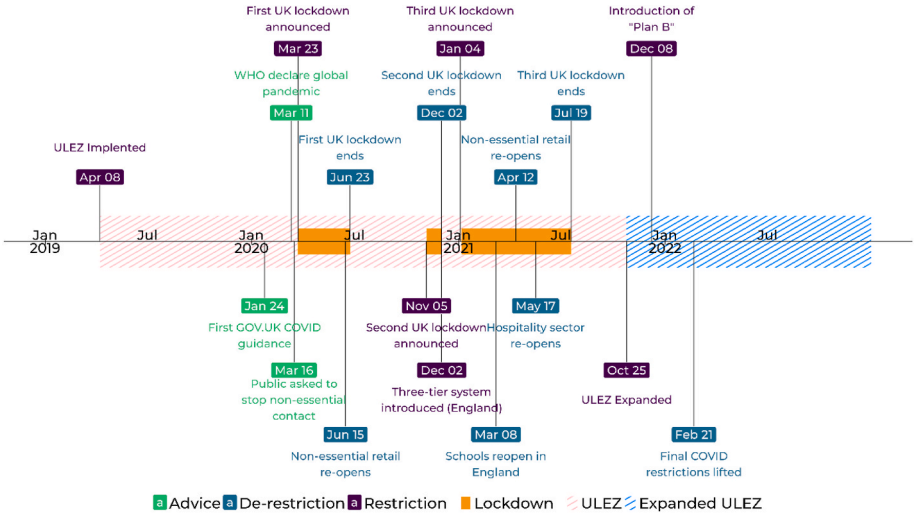

Fig. A1. Timeline of ULEZ and COVID-19 events between January 2019 and December 2020 (after Institute for Government, 2022; Sherrington, 2022; The Week, 2022).

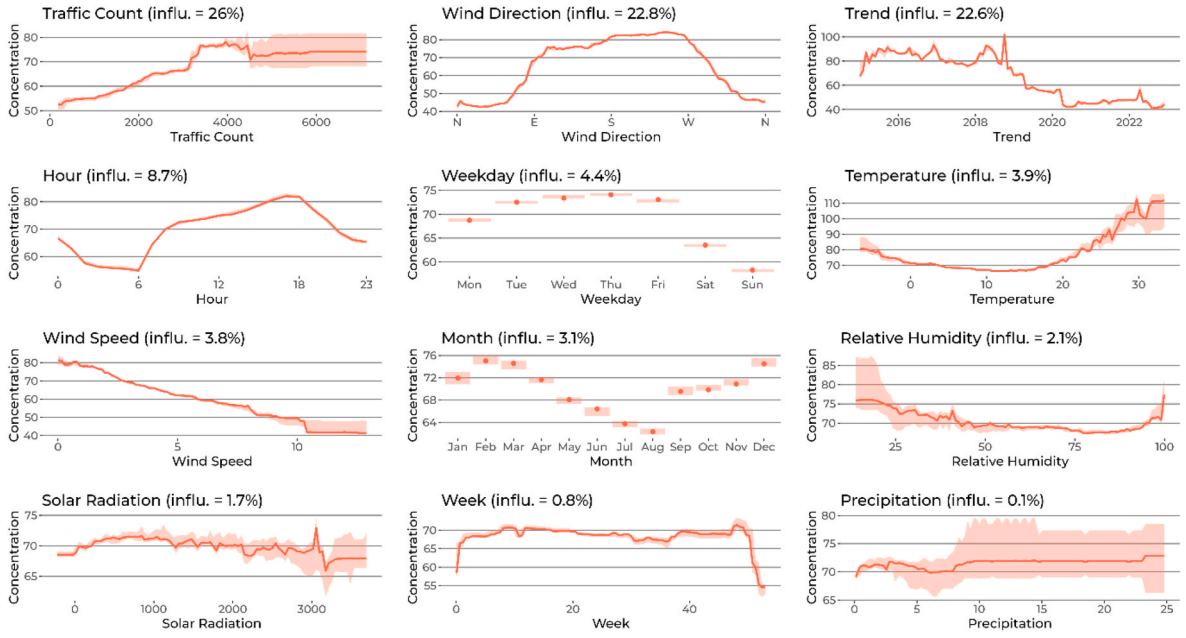

Fig. A2. Partial dependencies of NO_2 Gradient Boosted Regression model.

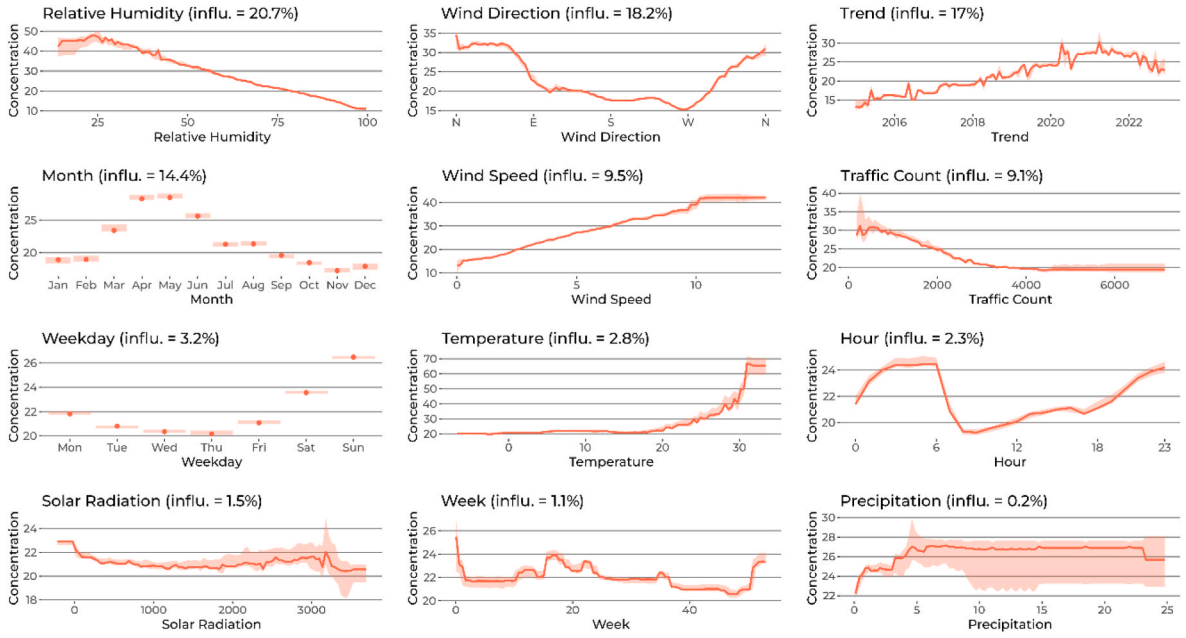

Fig. A3. Partial dependencies of O_3 Gradient Boosted Regression model.

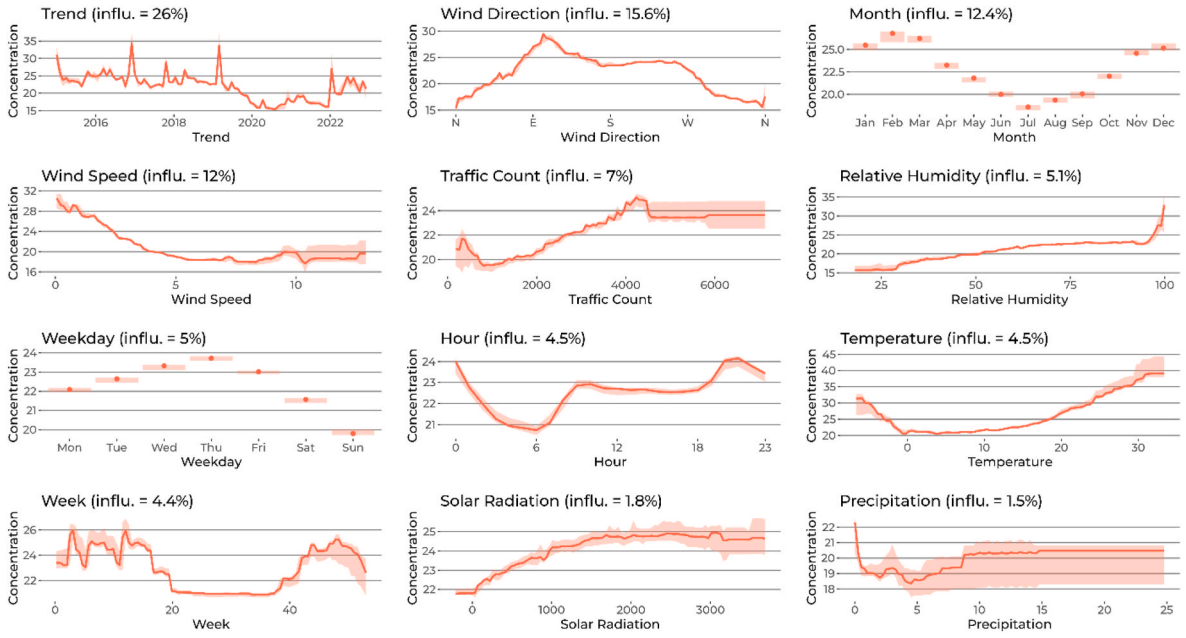

Fig. A4. Partial dependencies of PM_{10} Gradient Boosted Regression model.

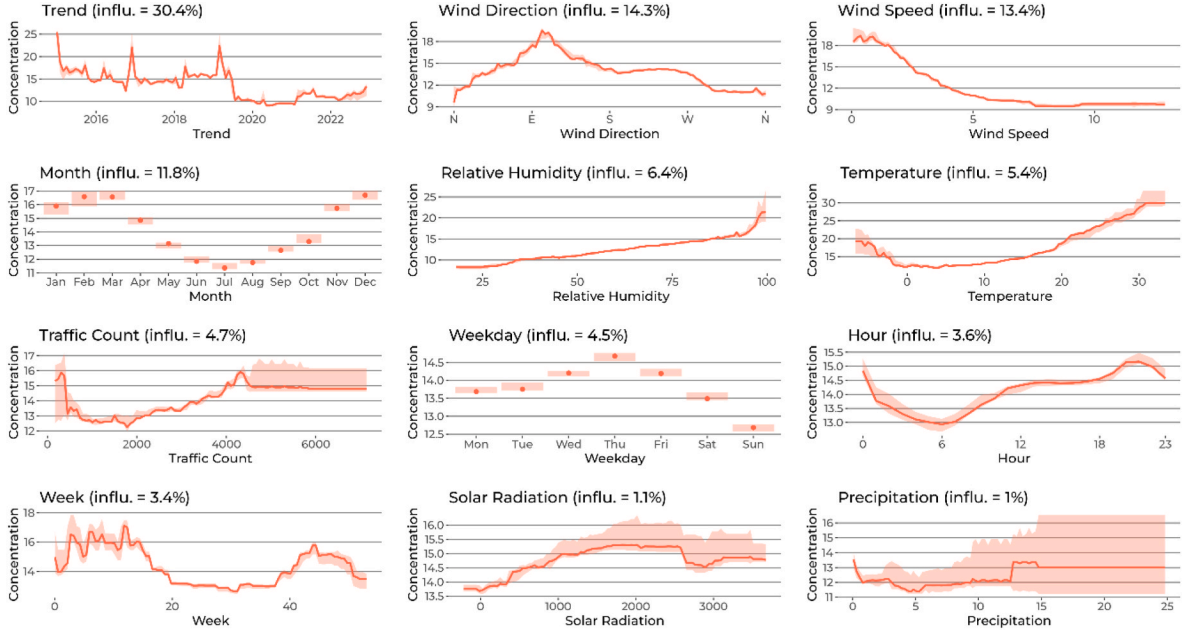

Fig. A5. Partial dependencies of $PM_{2.5}$ Gradient Boosted Regression model.

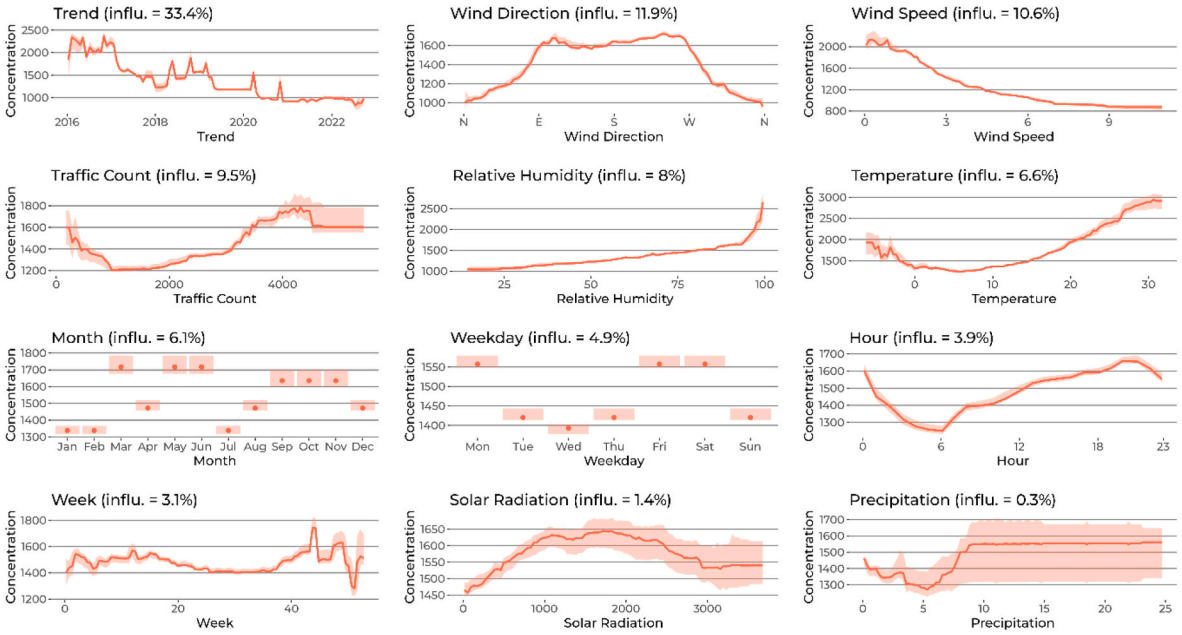

Fig. A6. Partial dependencies of accumulation Gradient Boosted Regression model.

Fig. A7. Partial dependencies of Aitken Gradient Boosted Regression model.

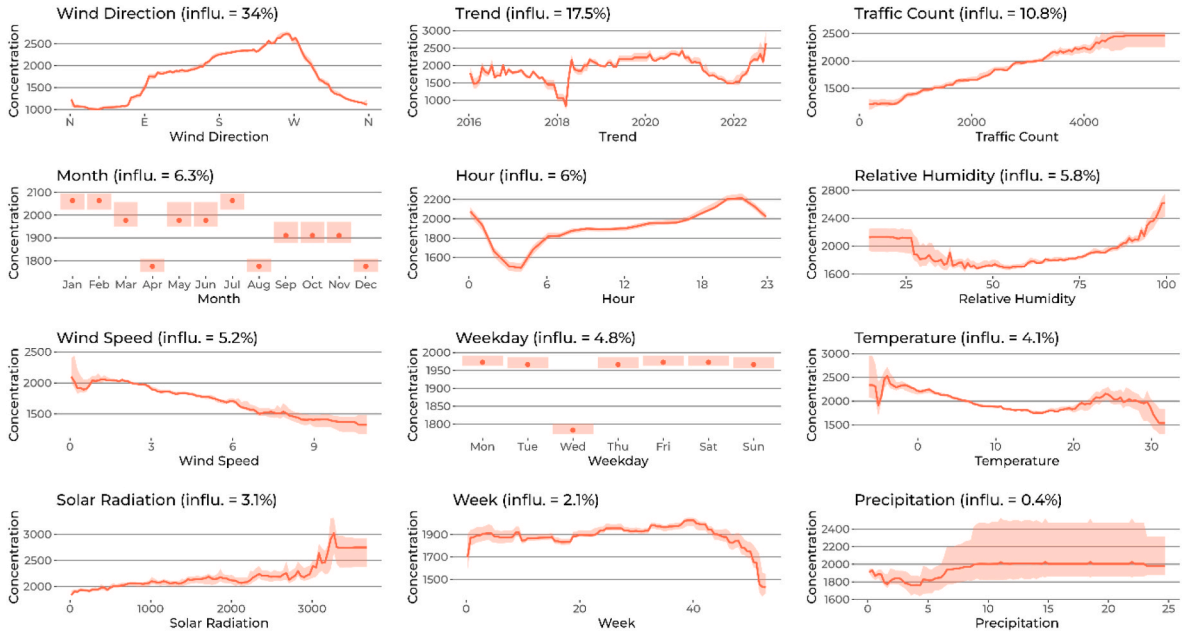

Fig. A8. Partial dependencies of nucleation Gradient Boosted Regression model.

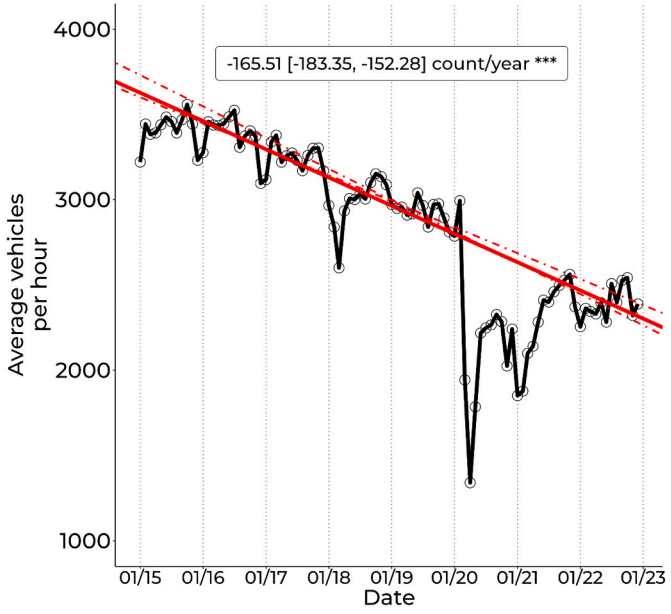

Fig. A9. Average hourly vehicle count between January 2015 and December 2022.

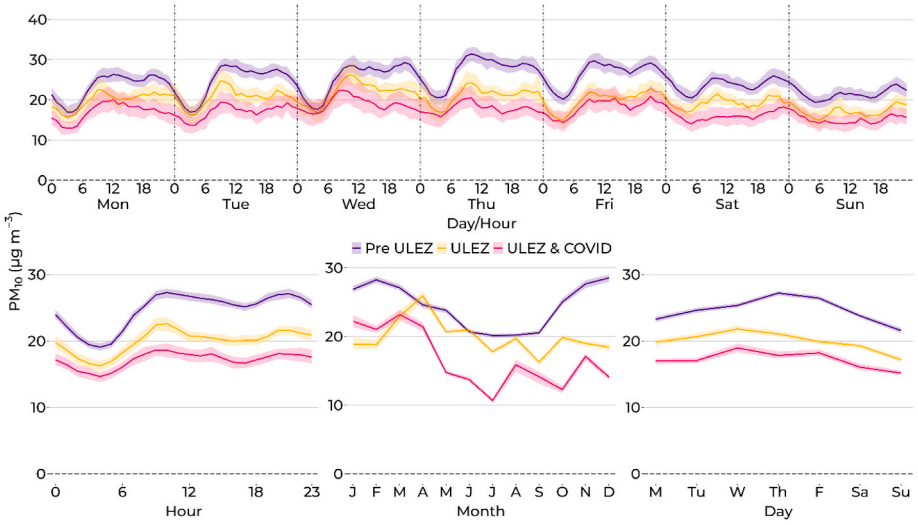

Fig. A10. Time variation plot of PM_{10} abundance across different interventions.

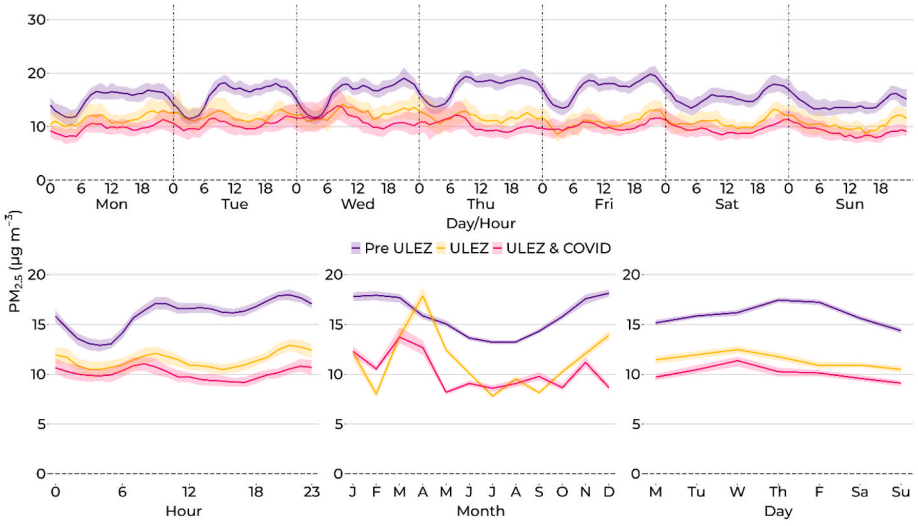

Fig. A11. Time variation plot of $PM_{2.5}$ abundance across different interventions.

Data availability

Data will be made available on request.

References

Addas, A., Maghrabi, A., 2021. The impact of COVID-19 lockdowns on air quality—A global review. Sustainability 13, 10212. https://doi.org/10.3390/su131810212.

Air Quality Expert Group, 2005. Particulate Matter in the United Kingdom. Department of the Environment, Food and Rural Affairs, London. https://uk-air.defra.gov.uk/library/assets/documents/reports/aqeg/Particulate_Matter_in_The_UK_2005.pdf. (Accessed 10 June 2022).

Anh, V., Duc, H., Azzi, M., 1997. Modeling anthropogenic trends in air quality data. J. Air Waste Manage. 47, 66–71. https://doi.org/10.1080/10473289.1997.10464406.

Araujo, J.A., Nel, A.E., 2009. Particulate matter and atherosclerosis: role of particle size, composition and oxidative stress. Part. Fibre Toxicol. 6, 24. https://doi.org/10.1186/1743-8977-6-24.

Boogaard, H., Janssen, N.A.H., Fischer, P.H., Kos, G.P.A., Weijers, E.P., Cassee, F.R., Van Der Zee, S.C., De Hartog, J.J., Meliefste, K., Wang, M., Brunekreef, B., Hoek, G., 2012. Impact of low emission zones and local traffic policies on ambient air pollution concentrations. Sci. Total Environ. 435–436. https://doi.org/10.1016/j.scitotenv.2012.06.089, 132–140.

Bousiotis, D., Pope, F.D., Beddows, D.C.S., Dall'Osto, M., Massling, A., Nøjgaard, J.K., Nordstrøm, C., Niemi, J.V., Portin, H., Petäjä, T., Perez, N., Alastuey, A., Querol, X., Kouvarakis, G., Mihalopoulos, N., Vratolis, S., Eleftheriadis, K., Wiedensohler, A., Weinhold, K., Merkel, M., Tuch, T., Harrison, R.M., 2021. A phenomenology of new particle formation (NPF) at 13 European sites. Atmos. Chem. Phys. 21, 11905–11925. https://doi.org/10.5194/acp-21-11905-2021.

Brown, J.S., Gordon, T., Price, O., Asgharian, B., 2013. Thoracic and respirable particle definitions for human health risk assessment. Part. Fibre Toxicol. 10, 12. https://doi.org/10.1186/1743-8977-10-12.

Carslaw, D., 2023a. Worldmet: import surface meteorological data from NOAA integrated surface database (ISD). https://CRAN.R-project.org/package=worldmet.

Carslaw, D., 2023b. Deweather: remove the influence of weather on air quality data. https://davidcarslaw.github.io/deweather/.

Carslaw, D., Ropkins, K., 2022. Openair — an R package for air quality data analysis. https://github.com/davidcarslaw/openair.

Carslaw, D.C., Taylor, P.J., 2009. Analysis of air pollution data at a mixed source location using boosted regression trees. Atmos. Environ. 43, 3563–3570. https://doi.org/10.1016/j.atmosenv.2009.04.001.

Cavallaro, F., Nocera, S., 2024. COVID-19 effects on transport-related air pollutants: insights, evaluations, and policy perspectives. Transp. Rev. 44, 484–517. https://doi.org/10.1080/01441647.2023.2225211.

Ceballos-Santos, S., González-Pardo, J., Carslaw, D.C., Santurtún, A., Santibáñez, M., Fernández-Olmo, I., 2021. Meteorological normalisation using boosted regression trees to estimate the impact of COVID-19 restrictions on air quality levels. IJERPH 18, 13347. https://doi.org/10.3390/ijerph182413347.

Chen, T., 2023. Foqat: field observation quick analysis toolkit. https://CRAN.R-project.org/package=foqat.

Ciupek, K., McGhee, E., Tompkins, J., Williams, K., Brown, A., Butterfield, D., Allerton, J., Bradshaw, C., Lilley, A., Kantilal, V., Robins, C., Sweeney, B., Brown, R., Priestman, M., Fuller, G., Green, D., Tremper, A., 2023. Airborne Particle

Concentrations, Particle Numbers and Black Carbon in the United Kingdom - Annual Report 2022. National Physical Laboratory, Teddington, UK. https://uk-air.defra.gov.uk/assets/documents/reports/cat09/2309281150_PCN_BC_Annual_Report_2022.pdf. (Accessed 13 March 2024).

Clapp, L., Jenkin, M., 2001. Analysis of the relationship between ambient levels of O_3, NO_2 and NO as a function of NOx in the UK. Atmos. Environ. 35, 6391–6405. https://doi.org/10.1016/S1352-2310(01)00378-8.

Conte, M., Dinoi, A., Grasso, F.M., Merico, E., Guascito, M.R., Contini, D., 2023. Concentration and size distribution of atmospheric particles in southern Italy during COVID-19 lockdown period. Atmos. Environ. 295, 119559. https://doi.org/10.1016/j.atmosenv.2022.119559.

Crapo, J.D., Barry, B.E., Chang, L., Mercer, R.R., 1984. Alterations in lung structure caused by inhalation of oxidants. J. Toxicol. Environ. Health 13, 301–321. https://doi.org/10.1080/15287398409530500.

Damayanti, S., Harrison, R.M., Pope, F., Beddows, D.C.S., 2023. Limited impact of diesel particle filters on road traffic emissions of ultrafine particles. Environ. Int. 174, 107888. https://doi.org/10.1016/j.envint.2023.107888.

De Jesus, A.L., Rahman, M.M., Mazaheri, M., Thompson, H., Knibbs, L.D., Jeong, C., Evans, G., Nei, W., Ding, A., Qiao, L., Li, L., Portin, H., Niemi, J.V., Timonen, H., Luoma, K., Petäjä, T., Kulmala, M., Kowalski, M., Peters, A., Cyrys, J., Ferrero, L., Manigrasso, M., Avino, P., Buonano, G., Reche, C., Querol, X., Beddows, D., Harrison, R.M., Sowlat, M.H., Sioutas, C., Morawska, L., 2019. Ultrafine particles and PM2.5 in the air of cities around the world: are they representative of each other? Environ. Int. 129, 118–135. https://doi.org/10.1016/j.envint.2019.05.021.

Department for Environment, 2022. Food and rural affairs, site information for London marylebone Road(UKA00315). https://uk-air.defra.gov.uk/networks/site-info?site_id=MY1. (Accessed 28 September 2022).

Department for Environment, Food and Rural Affairs, 2024. Standard Methods for Monitoring and UK Approach. Defra. UK. https://uk-air.defra.gov.uk/networks/monitoring-methods?view=eu-standards. (Accessed 1 November 2024).

Elith, J., Leathwick, J.R., Hastie, T., 2008. A working guide to boosted regression trees. J. Anim. Ecol. 77, 802–813. https://doi.org/10.1111/j.1365-2656.2008.01390.x.

Ellison, R.B., Greaves, S.P., Hensher, D.A., 2013. Five years of London's low emission zone: effects on vehicle fleet composition and air quality. Transport. Res. Transport Environ. 23, 25–33. https://doi.org/10.1016/j.trd.2013.03.010.

Feng, R., Xu, H., Wang, Z., Gu, Y., Liu, Z., Zhang, H., Zhang, T., Wang, Q., Zhang, Q., Liu, S., Shen, Z., Wang, Q., 2021. Quantifying air pollutant variations during COVID-19 lockdown in a capital city in Northwest China. Atmosphere 12, 788. https://doi.org/10.3390/atmos12060788.

Gómez-Losada, Á., Pires, J.C.M., 2024. Air quality assessment during the low emission zone implementation in Madrid (Spain). Urban Clim. 55, 101995. https://doi.org/10.1016/j.uclim.2024.101995.

Grange, S.K., Carslaw, D.C., 2019. Using meteorological normalisation to detect interventions in air quality time series. Sci. Total Environ. 653, 578–588. https://doi.org/10.1016/j.scitotenv.2018.10.344.

Greater London Authority, 2020. CENTRAL LONDON ULTRA LOW EMISSION ZONE – TEN MONTH REPORT. Greater London Authority, London, UK. https://www.london.gov.uk/sites/default/files/ulez_ten_month_evaluation_report_23_april_2020.pdf. (Accessed 18 September 2024).

Greater London Authority, 2024. LONDON-WIDE ULTRA LOW EMISSION ZONE – SIX MONTH REPORT. Greater London Authority, London, UK. https://www.london.gov.uk/sites/default/files/2024-07/London-wide%20ULEZ%20Six%20Month%20Report.pdf. (Accessed 18 September 2024).

Guo, S., Hu, M., Peng, J., Wu, Z., Zamora, M.L., Shang, D., Du, Z., Zheng, J., Fang, X., Tang, R., Wu, Y., Zeng, L., Shuai, S., Zhang, W., Wang, Y., Ji, Y., Li, Y., Zhang, A.L., Wang, W., Zhang, F., Zhao, J., Gong, X., Wang, C., Molina, M.J., Zhang, R., 2020. Remarkable nucleation and growth of ultrafine particles from vehicular exhaust. Proc. Natl. Acad. Sci. U.S.A 117, 3427–3432. https://doi.org/10.1073/pnas.1916366117.

Hajmohammadi, H., Heydecker, B., 2022. Evaluation of air quality effects of the London ultra-low emission zone by state-space modelling. Atmos. Pollut. Res. 13, 101514. https://doi.org/10.1016/j.apr.2022.101514.

Hama, S.M.L., Cordell, R.L., Kos, G.P.A., Weijers, E.P., Monks, P.S., 2017. Sub-micron particle number size distribution characteristics at two urban locations in Leicester. Atmos. Res. 194, 1–16. https://doi.org/10.1016/j.atmosres.2017.04.021.

Hao, J., Yin, Y., Li, X., Yuan, L., Xiao, H., 2015. Observations of nucleation mode particles formation and growth on mount huang, China. Procedia Eng. 102, 1167–1176. https://doi.org/10.1016/j.proeng.2015.01.242.

Hofman, J., Staelens, J., Cordell, R., Stroobants, C., Zikova, N., Hama, S.M.L., Wyche, K. P., Kos, G.P.A., Van Der Zee, S., Smallbone, K.L., Weijers, E.P., Monks, P.S., Roekens, E., 2016. Ultrafine particles in four European urban environments: results from a new continuous long-term monitoring network. Atmos. Environ. 136, 68–81. https://doi.org/10.1016/j.atmosenv.2016.04.010.

Holman, C., Harrison, R., Querol, X., 2015. Review of the efficacy of low emission zones to improve urban air quality in European cities. Atmos. Environ. 111, 161–169. https://doi.org/10.1016/j.atmosenv.2015.04.009.

Holmes, N.S., 2007. A review of particle formation events and growth in the atmosphere in the various environments and discussion of mechanistic implications. Atmos. Environ. 41, 2183–2201. https://doi.org/10.1016/j.atmosenv.2006.10.058.

Hong, G., Jee, Y.-K., 2020. Special issue on ultrafine particles: where are they from and how do they affect us? Exp. Mol. Med. 52, 309–310. https://doi.org/10.1038/s12276-020-0395-z.

Institute for Government, 2022. Timeline of UK Government Coronavirus Lockdowns and Restrictions. The Institute for Government. https://www.instituteforgovernment.org.uk/charts/uk-government-coronavirus-lockdowns. (Accessed 30 June 2022).

Jephcote, C., Hansell, A.L., Adams, K., Gulliver, J., 2021. Changes in air quality during COVID-19 'lockdown' in the United Kingdom. Environ. Pollut. 272, 116011. https://doi.org/10.1016/j.envpol.2020.116011.

Kamara, A.A., Harrison, R.M., 2021. Analysis of the air pollution climate of a central urban roadside supersite: london, marylebone road. Atmos. Environ. 258, 118479. https://doi.org/10.1016/j.atmosenv.2021.118479.

Kelly, F.J., Fussell, J.C., 2012. Size, source and chemical composition as determinants of toxicity attributable to ambient particulate matter. Atmos. Environ. 60, 504–526. https://doi.org/10.1016/j.atmosenv.2012.06.039.

Komppula, M., Lihavainen, H., Hatakka, J., Paatero, J., Aalto, P., Kulmala, M., Viisanen, Y., 2003. Observations of new particle formation and size distributions at two different heights and surroundings in subarctic area in northern Finland: new particle formation in northern Finland. J. Geophy. Res. 108. https://doi.org/10.1029/2002JD002939 n/a-n/a.

Kulmala, M., Kerminen, V.-M., Petäjä, T., Ding, A.J., Wang, L., 2017. Atmospheric gas-to-particle conversion: why NPF events are observed in megacities? Faraday Discuss 200, 271–288. https://doi.org/10.1039/C6FD00257A.

Kwon, H.-S., Ryu, M.H., Carlsten, C., 2020. Ultrafine particles: unique physicochemical properties relevant to health and disease. Exp. Mol. Med. 52, 318–328. https://doi.org/10.1038/s12276-020-0405-1.

Leathwick, J., Elith, J., Francis, M., Hastie, T., Taylor, P., 2006. Variation in demersal fish species richness in the oceans surrounding New Zealand: an analysis using boosted regression trees. Mar. Ecol. Prog. Ser. 321, 267–281. https://doi.org/10.3354/meps321267.

Lee, S., Gordon, H., Yu, H., Lehtipalo, K., Haley, R., Li, Y., Zhang, R., 2019. New particle formation in the atmosphere: from molecular clusters to global climate. JGR. Atmospheres 124, 7098–7146. https://doi.org/10.1029/2018JD029356.

Lee, J.D., Drysdale, W.S., Finch, D.P., Wilde, S.E., Palmer, P.I., 2020. UK surface NO2 levels dropped by 42 % during the COVID-19 lockdown: impact on surface O3. Atmos. Chem. Phys. 20, 15743–15759. https://doi.org/10.5194/acp-20-15743-2020.

Leighton, P.A., 1961. Photochemistry of Air Pollution. Academic Press, New York.

Lelieveld, S., Wilson, J., Dovrou, E., Mishra, A., Lakey, P.S.J., Shiraiwa, M., Pöschl, U., Berkemeier, T., 2021. Hydroxyl radical production by air pollutants in epithelial lining fluid governed by interconversion and scavenging of reactive oxygen species. Environ. Sci. Technol. 55, 14069–14079. https://doi.org/10.1021/acs.est.1c03875.

Li, J., Song, H., Luo, T., Cao, Y., Zhang, L., Zhao, Q., Li, Z., Hu, X., Gu, J., Tian, S., 2024. Exposure to O_3 and NO_2 on the interfacial chemistry of the pulmonary surfactant and the mechanism of lung oxidative damage. Chemosphere 362, 142669. https://doi.org/10.1016/j.chemosphere.2024.142669.

London borough of hounslow, ULEZ. https://www.hounslow.gov.uk/info/20053/transport/1939/ulez, 2022–. (Accessed 28 September 2022).

Ma, L., Graham, D.J., Stettler, M.E.J., 2021. Has the ultra low emission zone in London improved air quality? Environ. Res. Lett. 16, 124001. https://doi.org/10.1088/1748-9326/ac30c1.

Marinello, S., Butturi, M.A., Gamberini, R., 2021. How changes in human activities during the lockdown impacted air quality parameters: a review. Env. Prog. Sustain. 40. https://doi.org/10.1002/ep.13672.

Met Office, 2023a. MIDAS open: UK hourly rainfall data. v202308, 16164 Files, 5498350145 B. https://doi.org/10.5285/C21639861FB54623A749E502EBAC74ED.

Met Office, 2023b. MIDAS open: UK hourly solar radiation data. v202308, 5561 Files, 3017655306 B. https://doi.org/10.5285/87EB67C08F5C4518A3723D0CA2D9B4B1.

Miller, F.J., Gardner, D.E., Graham, J.A., Lee, R.E., Wilson, W.E., Bachmann, J.D., 1979. Size considerations for establishing a standard for inhalable particles. JAPCA 29, 610–615. https://doi.org/10.1080/00022470.1979.10470831.

Monks, P.S., Archibald, A.T., Colette, A., Cooper, O., Coyle, M., Derwent, R., Fowler, D., Granier, C., Law, K.S., Mills, G.E., Stevenson, D.S., Tarasova, O., Thouret, V., Von Schneidemesser, E., Sommariva, R., Wild, O., Williams, M.L., 2015. Tropospheric ozone and its precursors from the urban to the global scale from air quality to short-lived climate forcer. Atmos. Chem. Phys. 15, 8889–8973. https://doi.org/10.5194/acp-15-8889-2015.

Morawska, L., Thomas, S., Jamriska, M., Johnson, G., 1999. The modality of particle size distributions of environmental aerosols. Atmos. Environ. 33, 4401–4411. https://doi.org/10.1016/S1352-2310(99)00217-4.

Moreno-Ríos, A.L., Tejeda-Benítez, L.P., Bustillo-Lecompte, C.F., 2022. Sources, characteristics, toxicity, and control of ultrafine particles: an overview. Geosci. Front. 13, 101147. https://doi.org/10.1016/j.gsf.2021.101147.

Munir, S., Coskuner, G., Jassim, M.S., Aina, Y.A., Ali, A., Mayfield, M., 2021. Changes in air quality associated with mobility trends and meteorological conditions during COVID-19 lockdown in Northern England, UK. Atmosphere-Basel 12, 504. https://doi.org/10.3390/atmos12040504.

Mustafa, M.G., Elsayed, N.M., von Dohlen, F.M., Hassett, C.M., Postlethwait, E.M., Quinn, C.L., Graham, J.A., Gardner, D.E., 1984. A comparison of biochemical effects of nitrogen dioxide, ozone, and their combination in mouse lung. Toxicol. Appl. Pharmacol. 72, 82–90. https://doi.org/10.1016/0041-008X(84)90251-5.

Oberdörster, G., Sharp, Z., Atudorei, V., Elder, A., Gelein, R., Kreyling, W., Cox, C., 2004. Translocation of inhaled ultrafine particles to the brain. Inhal. Toxicol. 16, 437–445. https://doi.org/10.1080/08958370490439597.

Park, D., Lim, B.I., 2025. The effect of the ultra-low emission zone on PM2.5 concentration in Seoul, South Korea. Atmos. Environ. 340, 120908. https://doi.org/10.1016/j.atmosenv.2024.120908.

Peng, C., Deng, C., Lei, T., Zheng, J., Zhao, J., Wang, D., Wu, Z., Wang, L., Chen, Y., Liu, M., Jiang, J., Ye, A., Ge, M., Wang, W., 2023. Measurement of atmospheric nanoparticles: bridging the gap between gas-phase molecules and larger particles. J. Environ. Sci. 123, 183–202. https://doi.org/10.1016/j.jes.2022.03.006.

Potts, D.A., Marais, E.A., Boesch, H., Pope, R.J., Lee, J., Drysdale, W., Chipperfield, M.P., Kerridge, B., Siddans, R., Moore, D.P., Remedios, J., 2021. Diagnosing air quality changes in the UK during the COVID-19 lockdown using TROPOMI and GEOS-Chem. Environ. Res. Lett. 16, 054031. https://doi.org/10.1088/1748-9326/abde5d.

Poulhès, A., Proulhac, L., 2021. The Paris region low emission zone, a benefit shared with residents outside the zone. Transport. Res. Transport Environ. 98, 102977. https://doi.org/10.1016/j.trd.2021.102977.

R Core Team, 2024. R: a language and environment for statistical computing. https://www.R-project.org/.

Ridgeway, G., 2024. GBM developers, gbm: generalized boosted regression models. https://CRAN.R-project.org/package=gbm.

Ródenas, M., Soler, R., Borrás, E., Vera, T., Diéguez, J.J., Muñoz, A., 2022. Assessment of COVID-19 lockdown impact on the air quality in Eastern Spain: PM and BTX in urban, suburban and rural sites exposed to different emissions. Atmosphere-Basel 13, 97. https://doi.org/10.3390/atmos13010097.

Ropkins, K., Tate, J.E., 2021. Early observations on the impact of the COVID-19 lockdown on air quality trends across the UK. Sci. Total Environ. 754, 142374. https://doi.org/10.1016/j.scitotenv.2020.142374.

Santos, F.M., Gómez-Losada, Á., Pires, J.C.M., 2019. Impact of the implementation of Lisbon low emission zone on air quality. J. Hazard Mater. 365, 632–641. https://doi.org/10.1016/j.jhazmat.2018.11.061.

Schraufnagel, D.E., 2020. The health effects of ultrafine particles. Exp. Mol. Med. 52, 311–317. https://doi.org/10.1038/s12276-020-0403-3.

Shami, S., Ranjgar, B., Bian, J., Khoshlahjeh Azar, M., Moghimi, A., Amani, M., Naboureh, A., 2022. Trends of CO and NO_2 pollutants in Iran during COVID-19 pandemic using timeseries Sentinel-5 images in google Earth engine. Pollutants 2, 156–171. https://doi.org/10.3390/pollutants2020012.

Sherrington, A., 2022. 2 years of COVID-19 on GOV.UK – Government digital service. https://gds.blog.gov.uk/2022/07/25/2-years-of-covid-19-on-gov-uk/. (Accessed 17 September 2024).

Sillman, S., 1999. The relation between ozone, NOx and hydrocarbons in urban and polluted rural environments. Atmos. Environ. 33, 1821–1845. https://doi.org/10.1016/S1352-2310(98)00345-8.

Skirienė, A.F., Stasiškienė, Ž., 2021. COVID-19 and air pollution: measuring pandemic impact to air quality in five European countries. Atmosphere-Basel 12, 290. https://doi.org/10.3390/atmos12030290.

Spurny, K., 1998. On the physics, chemistry and toxicology of ultrafine anthropogenic, atmospheric aerosols (UAAA): new advances. Toxicol. Lett. 96–97, 253–261. https://doi.org/10.1016/S0378-4274(98)00080-0.

The Week, 2020. UK's covid timeline: key dates in the pandemic. Theweekuk. https://theweek.com/uk-news/107044/uk-coronavirus-timeline. (Accessed 17 September 2024).

Transport for London, FOI request detail. Request ID: FOI-1839-2122, transport for London. https://tfl.gov.uk/corporate/transparency/freedom-of-information/foi-request-detail?referenceId=FOI-1839-2122, 2021–. (Accessed 18 May 2024).

Transport for London, 2022a. Have your say: our proposals to help improve air quality, tackle the climate emergency and reduce congestion. Transp. London. London, UK. https://haveyoursay.tfl.gov.uk/15619/widgets/44946/documents/26977. (Accessed 28 September 2022).

Transport for London, ULEZ: where and when, transport for London. https://www.tfl.gov.uk/modes/driving/ultra-low-emission-zone/ulez-where-and-when, 2022–. (Accessed 28 September 2022).

Transport for London, FOI request detail. Request ID: FOI-1318-2324, transport for London. https://tfl.gov.uk/corporate/transparency/freedom-of-information/foi-request-detail?referenceId=FOI-1318-2324, 2023–. (Accessed 18 May 2024).

Transport for London, ways to meet the standard - transport for London. https://tfl.gov.uk/modes/driving/ultra-low-emission-zone/ways-to-meet-the-standard, 2024–. (Accessed 18 September 2024).

Transport for London, LEZ: where and when, transport for London. https://www.tfl.gov.uk/modes/driving/low-emission-zone/about-the-lez, 2025–. (Accessed 15 October 2025).

Vega, E., Namdeo, A., Bramwell, L., Miquelajauregui, Y., Resendiz-Martinez, C.G., Jaimes-Palomera, M., Luna-Falfan, F., Terrazas-Ahumada, A., Maji, K.J., Entwistle, J., Enríquez, J.C.N., Mejia, J.M., Portas, A., Hayes, L., McNally, R., 2021. Changes in air quality in Mexico City, London and Delhi in response to various stages and levels of lockdowns and easing of restrictions during COVID-19 pandemic. Environ. Pollut. 285, 117664. https://doi.org/10.1016/j.envpol.2021.117664.

von Bismarck-Osten, C., Birmili, W., Ketzel, M., Massling, A., Petäjä, T., Weber, S., 2013. Characterization of parameters influencing the spatio-temporal variability of urban particle number size distributions in four European cities. Atmos. Environ. 77, 415–429. https://doi.org/10.1016/j.atmosenv.2013.05.029.

Vu, T.V., Delgado-Saborit, J.M., Harrison, R.M., 2015. Review: particle number size distributions from seven major sources and implications for source apportionment studies. Atmos. Environ. 122, 114–132. https://doi.org/10.1016/j.atmosenv.2015.09.027.

Wehner, B., Uhrner, U., Von Löwis, S., Zallinger, M., Wiedensohler, A., 2009. Aerosol number size distributions within the exhaust plume of a diesel and a gasoline passenger car under on-road conditions and determination of emission factors. Atmos. Environ. 43, 1235–1245. https://doi.org/10.1016/j.atmosenv.2008.11.023.

Williams, M.L., Atkinson, R.W., Anderson, H.R., Kelly, F.J., 2014. Associations between daily mortality in London and combined oxidant capacity, ozone and nitrogen dioxide. Air Qual. Atmos. Health 7, 407–414. https://doi.org/10.1007/s11869-014-0249-8.

World Health Organisation, 2021. WHO global air quality guidelines: particulate matter (PM2. 5 and PM10), ozone, nitrogen dioxide. Sulfur Dioxide and Carbon Monoxide. World Health Organization, Geneva. https://iris.who.int/bitstream/handle/10665/345329/9789240034228-eng.pdf?sequence=1. (Accessed 14 July 2025).

Wu, Z., Hu, M., Lin, P., Liu, S., Wehner, B., Wiedensohler, A., 2008. Particle number size distribution in the urban atmosphere of Beijing, China, Atmos. Environ. Times 42, 7967–7980. https://doi.org/10.1016/j.atmosenv.2008.06.022.

Wyche, K.P., Nichols, M., Parfitt, H., Beckett, P., Gregg, D.J., Smallbone, K.L., Monks, P. S., 2021. Changes in ambient air quality and atmospheric composition and reactivity in the South East of the UK as a result of the COVID-19 lockdown. Sci. Total Environ. 755, 142526. https://doi.org/10.1016/j.scitotenv.2020.142526.

Xiao, M., Hoyle, C.R., Dada, L., Stolzenburg, D., Kürten, A., Wang, M., Lamkaddam, H., Garmash, O., Mentler, B., Molteni, U., Baccarini, A., Simon, M., He, X.-C., Lehtipalo, K., Ahonen, L.R., Baalbaki, R., Bauer, P.S., Beck, L., Bell, D., Bianchi, F., Brilke, S., Chen, D., Chiu, R., Dias, A., Duplissy, J., Finkenzeller, H., Gordon, H., Hofbauer, V., Kim, C., Koenig, T.K., Lampilahti, J., Lee, C.P., Li, Z., Mai, H., Makhmutov, V., Manninen, H.E., Marten, R., Mathot, S., Mauldin, R.L., Nie, W., Onnela, A., Partoll, E., Petäjä, T., Pfeifer, J., Pospisilova, V., Quéléver, L.L.J., Rissanen, M., Schobesberger, S., Schuchmann, S., Stozhkov, Y., Tauber, C., Tham, Y. J., Tomé, A., Vazquez-Pufleau, M., Wagner, A.C., Wagner, R., Wang, Y., Weitz, L., Wimmer, D., Wu, Y., Yan, C., Ye, P., Ye, Q., Zha, Q., Zhou, X., Amorim, A., Carslaw, K., Curtius, J., Hansel, A., Volkamer, R., Winkler, P.M., Flagan, R.C., Kulmala, M., Worsnop, D.R., Kirkby, J., Donahue, N.M., Baltensperger, U., El Haddad, I., Dommen, J., 2021. The driving factors of new particle formation and growth in the polluted boundary layer. Atmos. Chem. Phys. 21, 14275–14291. https://doi.org/10.5194/acp-21-14275-2021.

Xin, Y., Shao, S., Wang, Z., Xu, Z., Li, H., 2021. COVID-2019 lockdown in Beijing: a rare opportunity to analyze the contribution rate of road traffic to air pollutants. Sustain. Cities Soc. 75, 102989. https://doi.org/10.1016/j.scs.2021.102989.

Zhang, R., Khalizov, A., Wang, L., Hu, M., Xu, W., 2012. Nucleation and growth of nanoparticles in the atmosphere. Chem. Rev. 112, 1957–2011. https://doi.org/10.1021/cr2001756.